COMBINING STEAM-METHANE REFORMING, WATER-GAS SHIFT, AND CO_2 REMOVAL IN A SINGLE-STEP PROCESS FOR HYDROGEN PRODUCTION

Final Report

For Period March 15, 1997 -- December 14, 2000

Alejandro Lopez Ortiz
Bhaskar Balasubramanian
Douglas P. Harrison

Louisiana State University
Baton Rouge, Louisiana 70803

February 2001

Prepared for

THE U. S. DEPARTMENT OF ENERGY
AWARD NO. DE-FG02-97ER12208

DISCLAIMER

NOTICE

COMBINING STEAM-METHANE REFORMING, WATER-GAS SHIFT, AND CO_2 REMOVAL IN A SINGLE-STEP PROCESS FOR HYDROGEN PRODUCTION

OBJECTIVE

The objective of the research project was to determine the feasibility of a simpler, more energy efficient process for the production of 95+% H_2 from natural gas, and to collect sufficient experimental data on the effect of reaction parameters to guide additional larger-scale process development.

INTRODUCTION

Hydrogen has long been an important raw material for the chemical and petroleum industries. Large quantities are used in the manufacture of ammonia and methanol and in a range of petroleum refining hydrotreating processes. A growing demand is forecast, particularly if hydrogen emerges as a general-purpose energy source for space heating, electric power generation, and transportation fuel.

Conversion of natural gas and other light hydrocarbons via steam reforming is the major process for H_2 production, and the H_2 content of the product may range from 95% to greater than 99.9%. Heavier hydrocarbons may be converted to H_2 by partial oxidation, while coal and petroleum coke may serve as raw materials in the future. Non-hydrocarbon processes, such as water electrolysis, may also be used to produce H_2, while H_2 production from renewable resources is currently under study. The cost of electrolytic H_2 is almost twice that of H_2 from natural gas, while H_2 from renewable resources is not expected to become competitive for another 30 to 40 years (U.S. DOE, 1995). Thus steam-methane reforming will likely remain the process of choice for the next few decades. Although steam-methane technology is mature, significant process improvements may be possible.

CONVENTIONAL STEAM-METHANE REFORMING

The first step of the conventional process involves the highly endothermic reaction between natural gas (represented here as CH_4) and steam over a nickel catalyst.

$$CH_4(g) + H_2O(g) \leftrightarrow CO(g) + 3H_2(g) \qquad (1)$$

Large quantities of supplemental fuel are needed to maintain reaction conditions of about 850°C and 15 atm. The reformer product enters a two-stage shift reactor where additional H_2 is formed by the reaction

$$CO(g) + H_2O(g) \leftrightarrow CO_2(g) + H_2(g) \qquad (2)$$

This reaction is moderately exothermic and dual catalyst beds with interbed cooling are normally employed to prevent overheating and to promote complete conversion of CO.

CO_2 is removed by, for example, absorption into an amine solvent. The solvent is regenerated by steam stripping and continually recycled between the absorber and stripper. Stripped CO_2 is normally discharged to the atmosphere. Small quantities of CO and CO_2 remaining in the product may be converted back to CH_4 via the reactions

$$CO(g) + 3H_2(g) \leftrightarrow CH_4(g) + H_2O(g) \quad (3)$$

$$CO_2(g) + 4H_2(g) \leftrightarrow CH_4(g) + 2H_2O(g) \quad (4)$$

Remaining H_2O is removed to produce a final product having a H_2 content of 95+%. CH_4 is the major impurity and only ppm concentrations of carbon oxides are present.

Extremely high purity H_2 ($\geq$99.9%) may be produced by substituting pressure swing adsoprtion (PSA) for the CO_2 scrubbing and methanation steps. The disadvantage of PSA is that approximately 20% of the H_2 is lost during column blowdown and purge. This PSA off-gas is normally routed back to the fuel side of the reformer to replace a portion of the natural gas fuel required to maintain reformer temperature.

In a recent review, Adris et al. (1996) identified three areas in which research could result in significant improvement in the steam methane reforming process: (1) improved catalysts for higher activity and mechanical strength, and better resistance to carbon deposition and sulfur poisoning, and alternate catalyst shapes to increase the effectiveness factor; (2) improved reformer tube materials better able to withstand high temperatures and high thermal flux; and (3) alternate reactor configurations not requiring reformer tubes.

The alternate H_2 process studied in this research project is potentially simpler and less energy intensive that the conventional process. The problems identified by Adris et al. (1996) are either avoided or significantly reduced in importance.

SINGLE-STEP PROCESS

In the single-step process, the reforming, shift, and CO_2 removal steps are combined in a single reactor vessel. The simultaneous reactions are

$$CH_4(g) + H_2O(g) \leftrightarrow CO(g) + 3H_2(g) \quad (1)$$

$$CO(g) + H_2O(g) \leftrightarrow CO_2(g) + H_2(g) \quad (2)$$

$$CO_2(g) + CaO(s) \leftrightarrow CaCO_3(s) \quad (5)$$

Natural gas and steam are fed to the reactor that contains both reforming catalyst and CaO-based acceptor for CO_2 removal. Heat released by the exothermic shift and carbonation reactions is approximately equal to the heat required for endothermic reforming so that, with proper heat integration, no supplemental energy is required. Removal of CO_2 from the gas phase as it is formed upsets the normal equilibrium limits

and allows both the reforming and shift reactions to proceed almost to completion. 95+% H_2 can be produced in this single step. Additional processing may be required to produce extremely high purity H_2 or to reduce carbon oxide concentrations.

For economic reasons it will be necessary to regenerate the CO_2 acceptor according to the reverse of reaction (5) so that the acceptor may be used for many reaction-regeneration cycles. In large-scale continuous steady-state operation dual circulating fluidized beds may be used. The regeneration reactor is analagous to the CO_2 stripper in the standard process, and supplemental energy is required for regeneration. However, as shown in a later section of this report, about 20% to 25% less supplemental energy is required for acceptor regeneration than is currently needed in the reforming furnace. In smaller-scale applications, dual fixed-bed reactors may be used with the combined reactions occurring in one bed while regeneration occurs in the other. When the acceptor in the primary reactor is consumed and regeneration is complete, gas flow is reversed and the process continues.

RELATED RESEARCH

The concept of combining reaction and separation to simplify chemical processes, conserve energy, and/or to improve product quality and yield has received increased attention for a number of years. Reactive distillation is an example that has been commercialized, while the use of catalytic membrane reactors for equilibrium-limited reactions is the subject of much current research.

The single-step process for H_2 production may be described generically as sorption enhanced reaction. The concept is not new. Rostrup-Nielsen (1984) reports that the first description of the conversion of hydrocarbons in the presence of steam and a CO_2 acceptor was published in 1868. Williams (1933) was issued a patent for a process in which steam and methane react in the presence of a mixture of lime and catalyst to produce H_2. Gorin and Retallick (1963) patented a fluidized-bed process using reforming catalyst and CO_2 acceptor. Brun-Tsekhovoi et al (1988) showed that the combined reaction equilibrium could be closely approached at 625°C, 2 MPa, and space velocities as large as 12,000hr^{-1}.

More recently, Han and Harrison (1994, 1997) in this laboratory studied the combined shift and carbonation reactions for the production of H_2 from synthesis gas. Air Products and Chemicals, Inc. (APCI) has studied the single-step production of H_2 from natural gas by combining reforming catalyst with a K_2CO_3-treated hydrotalcite acceptor for CO_2 removal (Anand et al. 1996, Mayorga et al. 1997). Energy and Environmental Research Corporation (EERC) (Kumar et al. 1999) has reported research results on a process referred to as Unmixed Combustion (UMC) which is similar to the single-step process studied here.

The ZECA (Zero Emission Coal Alliance) project being developed at Los Alamos National Laboratory (Ziock and Lackner, 2001) depends on a calcium-based acceptor to remove CO_2 as one step in an overall process designed to utilize the energy from coal

with no atmospheric emissions of CO_2, H_2S, NO_x or particulates. A similar process that utilizes the calcium-based CO_2 acceptor, called HyPr-Ring is under development in Japan (Hatano et al. 2001).

THERMODYNAMIC ANALYSIS

The potential advantages of combining reaction and separation for H_2 production can be understood from a thermodynamic analysis of the important reactions. The thermodynamic program HSC Chemistry (Roine, 1999) was used for equilibrium calculations. As will be shown later, the combined reactions are quite fast so that equilibrium calculations provide an accurate estimate of experimental results at most reaction conditions of interest.

Figures 1 and 2 show, respectively, the equilibrium H_2 content and hydrogen production rate (mol H_2 produced per mol of CH_4 fed), both on a dry basis, as a function of temperature and pressure for the combined reforming, shift, and carbonation reactions. The initial composition used in these calculations consisted of CH_4, H_2O, and CaO in a molar ration of 1:4:2. The rather complex response of the thermodynamics is due to the contrasting effects of temperature and pressure on the individual reactions. Reforming (reaction 1) is endothermic and involves an increase in the number of gas phase mols. Hence, high temperature and low pressure favor this reaction. Both the shift (reaction 2) and carbonation reactions (reaction 5) are exothermic, and high equilibrium conversion is favored by low temperature. The shift reaction involves no change in gas phase mols and is, therefore, independent of pressure. Carbonation produces a decrease in gas phase mols and is favored by high pressure.

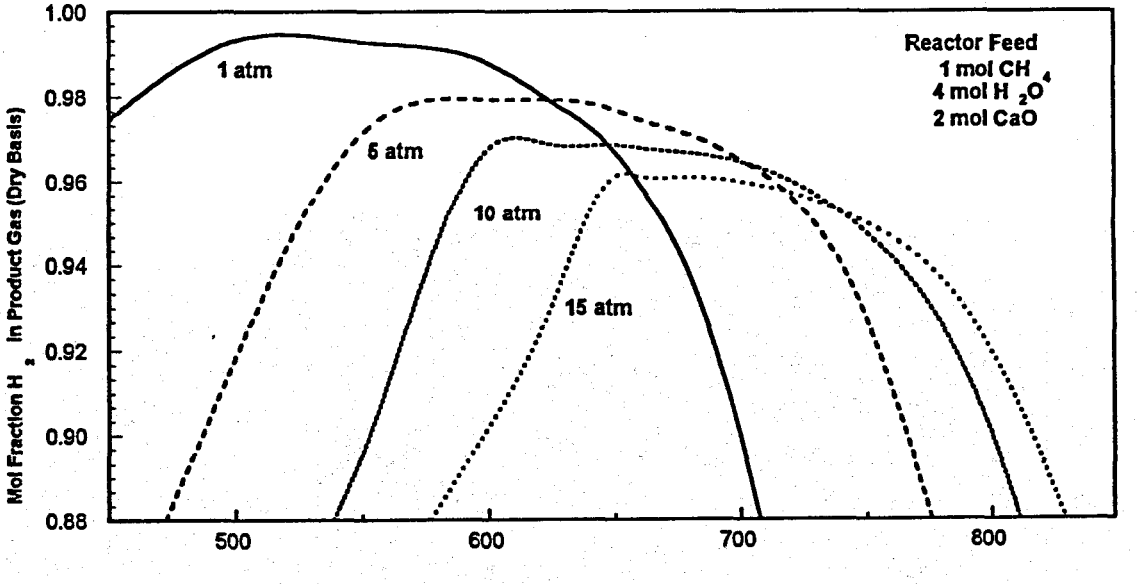

Figure 1. Equilibrium Mol Fraction H_2 (Dry Basis) as a Function of Temperature and Pressure

Maximum H_2 content and H_2 production rate occur at low pressure and low temperature. At 500°C and 1 atm it is theoretically possible to produce 99% H_2 (dry basis) at a rate of 3.9 mol H_2 per mol of CH_4. However, the economics of large-scale H_2 production require higher pressures in the range of 15 to 20 atm even though the H_2 purity and yield are lower. It is clear, however, from Figure 1 that 95+% H_2 can theoretically be produced over a relatively wide range of temperatures and pressures. The majority of the experimental studies were conducted at 650°C and 15 atm where it is possible to produce 96% H_2 at a rate of 3.5 mol H_2 per mol of CH_4.

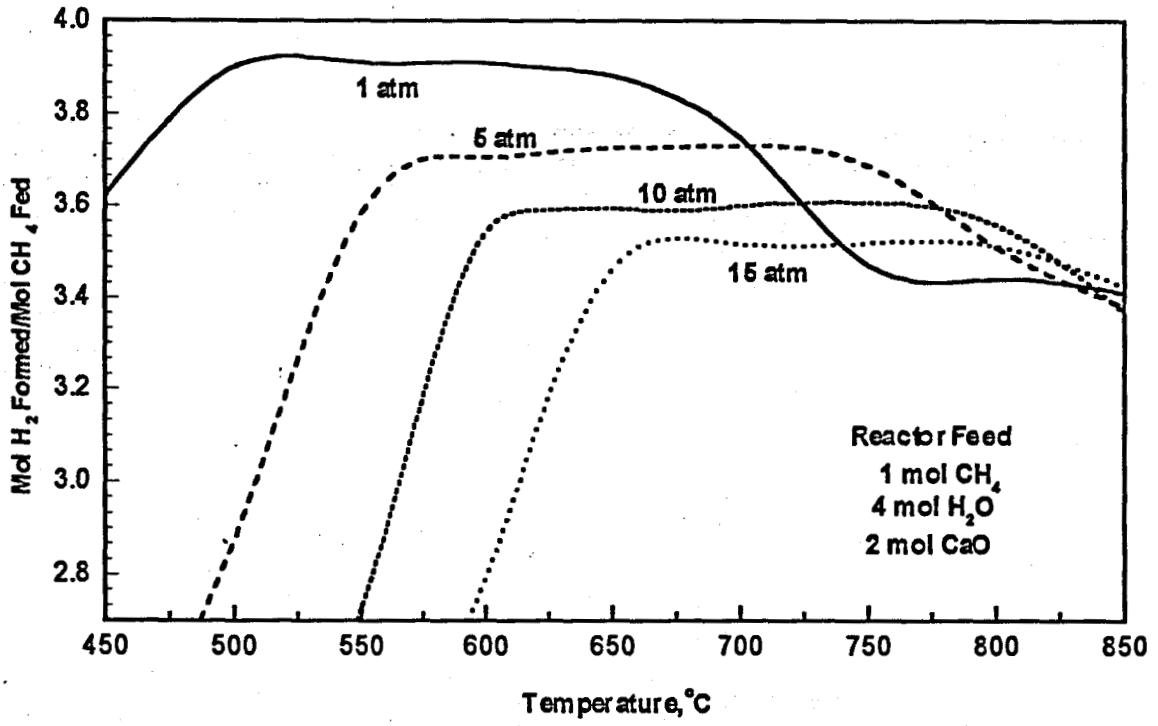

Figure 2. Equilibrium Hydrogen Production Rate as a Function of Temperature and Pressure

Equilibrium H_2 concentration with and without the CaO-based acceptor is compared in Figure 3 as a function of temperature at fixed pressure of 15 atm. In the conventional process (without acceptor) the H_2 concentration increases with increasing temperature, which is consistent with the endothermic reforming reaction. The thermal neutrality of the combined reactions with acceptor is illustrated by the relative constancy of the H_2 content and production rate at temperatures below 750°C. At higher temperatures the ability of the acceptor to remove CO_2 begins to decrease. No carbonation is possible above about 875°C at 15 atm and the thermodynamics of both the conventional and single-step processes are identical.

Two branches are shown in Figure 3 in the equilibrium H_2 content curve with acceptor below 600°C due to the possible formation of $Ca(OH)_2$ by the reaction

$$CaO(s) + H_2O(g) \leftrightarrow Ca(OH)_2(s) \qquad (6)$$

In the lower branch, the thermodynamic analysis allowed for the formation of both $CaCO_3$ and $Ca(OH)_2$, while $Ca(OH)_2$ was excluded from the possible equilibrium products in the upper branch. $Ca(OH)_2$ formation is not possible above about 600°C at 15 atm in that gas composition. $Ca(OH)_2$ formation is detrimental to the process in two ways. First, it reduces the amount of calcium available to react with CO_2 and, secondly, it reduces the amount of H_2O needed to drive the reforming and shift reactions. Because of the limited number of experimental tests conducted below 650°C, the actual importance of $Ca(OH)_2$ formation has not been fully defined.

At the standard experimental reaction temperature of 650°C, the single step process is capable of producing 96% H_2 (dry basis) while the maximum H_2 content from the conventional reformer at this temperature is about 65% (dry basis). Feeding 65% H_2 to a two-stage shift reactor and CO_2 scrubber would only increase the H_2 content to 88%. At 850°C the H_2 content from the conventional reformer is slightly less than 80% and two stages of shift reaction followed by CO_2 removal are required to reach 95+% H_2.

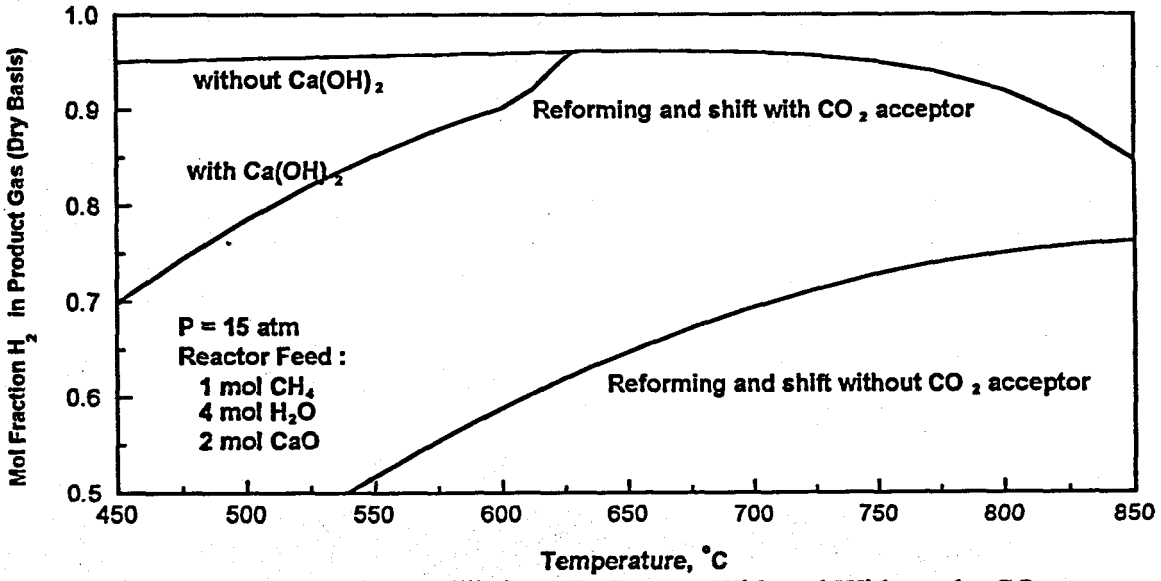

Figure 3. Comparison of the Equilibrium H_2 Content With and Without the CO_2 Acceptor

The equilibrium composition of the impurities in the H_2 product from the single-step process is a strong function of temperature as shown in Figure 4. At lower temperatures essentially all of the carbon oxides ($CO + CO_2$) are removed and the primary impurity is unreacted CH_4. In contrast, the conversion of CH_4 increases at higher temperature while CO_2 removal efficiency decreases, and the primary impurities become CO and CO_2. The ability to produce low-CO H_2 in the single-step process at lower temperatures may be particularly significant if the H_2 is to be used in a catalytic process such as PEM fuel cells. CO is a poison for the platinum anode catalyst and an additional processing step, preferential oxidation, is required after the second shift reactor to meet

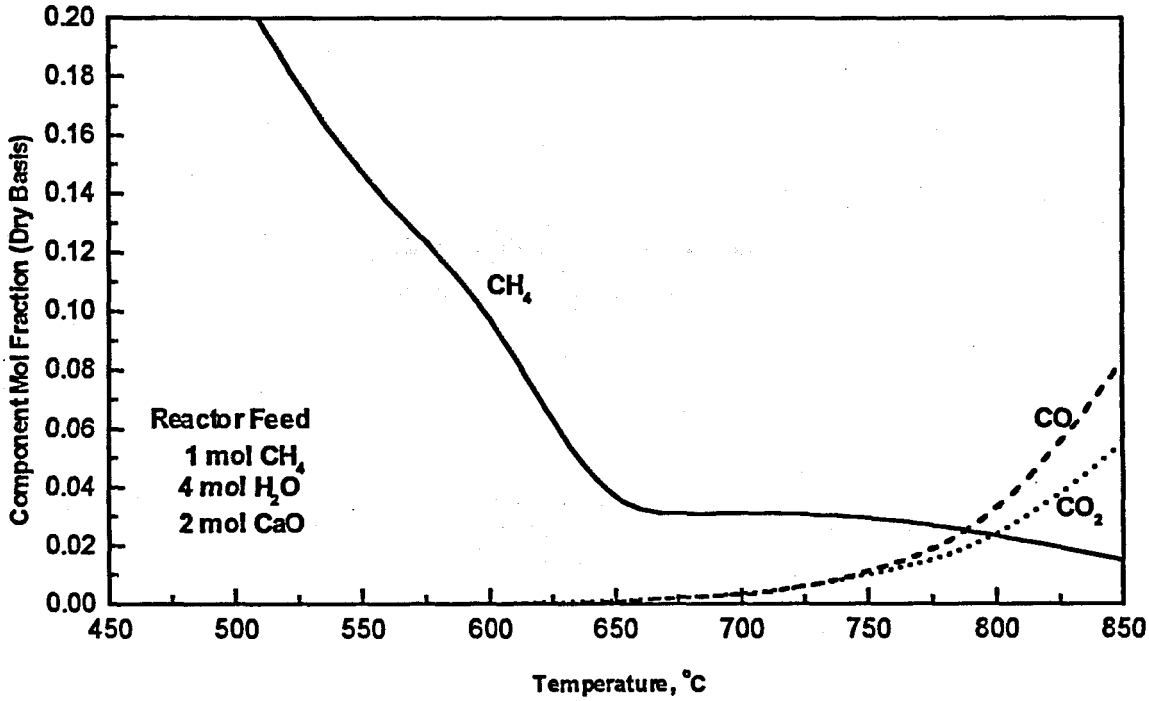

Figure 4. Equilibrium Impurities in the H_2 Product at 15 atm

CO specifications. In the single-step process it is theoretically possible to reduce the CO content to less than 20ppmv at 500°C.

Acceptor regeneration requires the addition of supplemental energy to increase the temperature to the level that $CaCO_3$ will decompose according to the reverse of reaction (5). Figure 5 shows the equilibrium CO_2 pressure over CaO as a function of temperature. CaO carbonation is thermodynamically favored at temperatures and pressures above and to the left of the line while $CaCO_3$ decomposition is favored below and to the right of the line. Regeneration is favored at all temperatures shown in a CO_2-free atmosphere. However, temperatures near 800°C are needed to achieve rapid decomposition kinetics. Decomposition will occur in pure CO_2 at one atm at about 900°C, while 1115°C is required for decomposition in pure CO_2 at 15 atm. The Figure 5 results were used to select regeneration temperatures used in the experimental program, which ranged from 800°C to 950°C.

PROCESS SIMULATION

Process simulation studies using Aspen-Plus were carried out to confirm the potential advantages of the single-step H_2 process. Detailed material and energy balance calculations were made for three case studies: (1) the conventional steam-methane process; (2) the single-step process using direct heating for acceptor regeneration with no CO_2 control; and (3) the single-step process using indirect heating and production of pure, sequestration-ready CO_2 regenerator off-gas. All simulations were based on chemical

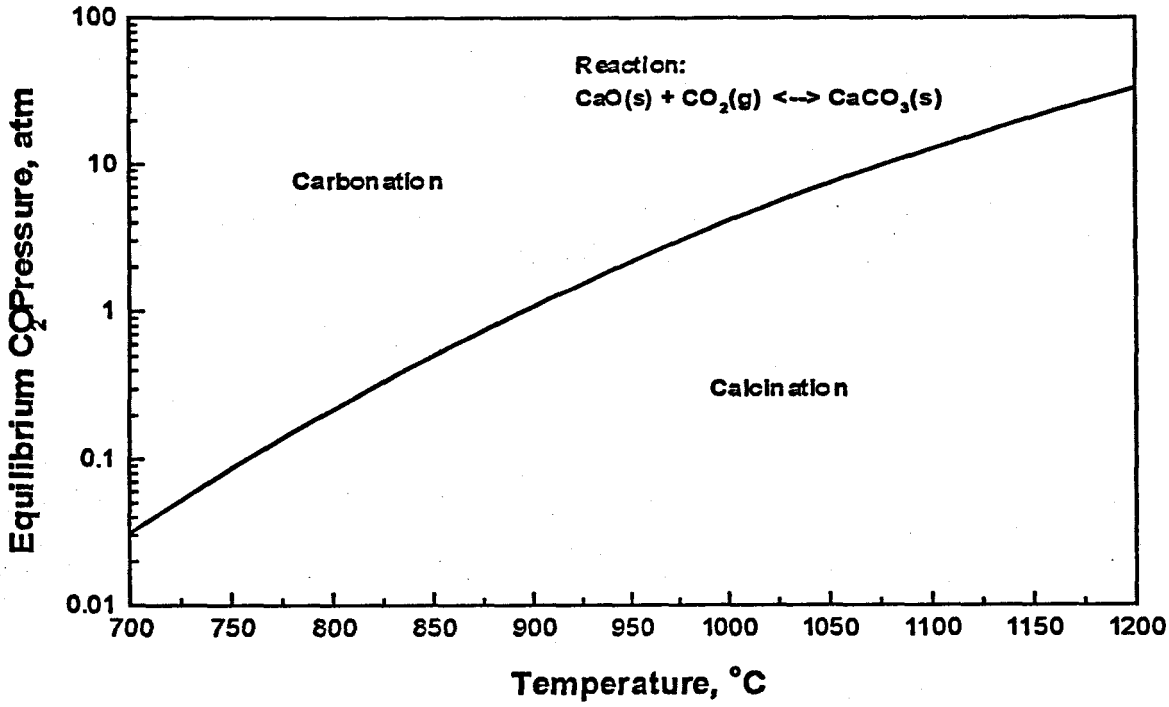

Figure 5. Equilibrium CO_2 Pressure as a Function of Temperature.

equilibrium. Only a brief summary of the results is presented in this report. Additional details may be found in Lopez' (2000) dissertation.

The conventional process simulation employed a reforming furnace, two shift reactors, and an amine CO_2 separation plant. Compressors, pumps, heat exchangers, etc. were included in the detailed process flow diagram. Material and energy balances were based on 1 mol of process CH_4 feed (not including supplemental fuel) and 4 mols of H_2O (steam/carbon = 4). The reformer operated at 850°C and 15 atm, while the two shift reactors operated adiabatically with feed and exit temperatures to the high and low temperature shift reactors of 366°C and 420°C, and 229°C and 250°C, respectively. Excess water was removed by condensation and CO_2 was removed by scrubbing with a monoethanolamine (MEA) solution. The pressure of the CO_2-rich amine solution was reduced to 1 atm and CO_2 was removed by steam stripping at about 100°C. 3.72 mol of 97.9% H_2 product exited from the top of the amine scrubber. Product impurities consisted of 1.6% unreacted CH_4, 0.5% H_2O and small amounts of CO and CO_2. 0.51 mol of supplemental CH_4 fuel were burned with 10% excess air to provide the energy required by the reformer, and 0.77 mols of export superheated steam were generated as a by-product by heat exchange with the reformer product gas.

The single-step process was simulated using two options for acceptor regeneration. In the first, regeneration energy was added by combustion of supplemental CH_4 using 10% excess air in direct contact with the spent acceptor and reforming catalyst. Liberated CO_2 in this option was diluted with combustion products and

discharged to the atmosphere. In the second option, regeneration energy was added to a stream of circulating CO_2 via indirect heating. The regenerator gas product of pure CO_2 was then split with one portion recycled to the heater and regenerator and the remainder available for sequestration.

In the direct heat option, the feed to the primary fluidized-bed reactor consisted of 4 mol of H_2O and 1 mol of CH_4 (the same steam-to-methane ratio as used for the conventional process simulation). Solid acceptor consisted of 1.75 mol of calcined dolomite (1.75 mol of CaO and 1.75 mol of MgO), 75% excess CaO based on complete conversion of CH_4 to CO_2. Catalyst feed consisted of 0.173 mol of NiO and 0.425 mol of Al_2O_3 support (23 wt% NiO) to produce a 3-to-1 mass ratio of acceptor to catalyst, approximately equal to the ratio used in the experimental tests. Reduction of NiO to active Ni occurred in the primary reactor. The solid circulation rate was fixed so that no supplemental energy was required in the primary reactor, which operated at 650°C and 15 atm. Spent acceptor and catalyst were transferred to the fluidized-bed regenerator where $CaCO_3$ was decomposed to CaO at 15 atm and 972°C, with the required energy supplied by burning 0.39 mol of CH_4 with 10% excess air in direct contact with the acceptor-catalyst mixture. 3.36 mols of 96.5% product H_2 were produced directly in the primary reactor. Impurities consisted of 3.3% unreacted CH_4, and about 0.1% CO and CO_2. If lower carbon oxide concentrations are needed, the product gas could be further purified by methanation. High-pressure regenerator off-gas was used to drive the air compressor and provide of export power.

The production of pure CO_2 off-gas for greenhouse gas control purposes using the single-step process was also studied. Primary reactor feed again consisted of 1 mol of CH_4 and 4 mol of H_2O. Reactor temperature was again 650°C but pressure was reduced to 3 atm so that regeneration in pure CO_2 could also be accomplished at 972°C. The product gas contained 97.7% H_2 (dry basis) at a production rate of 3.79 mol H_2 per mol of CH_4 feed. Impurities consisted of 1.2% unreacted CH_4 and about 1% CO plus CO_2. The solid circulation rate of 1.2 mol of calcined dolomite and 0.41 mol of catalyst was fixed so that no supplemental energy was required in the primary reactor. This rate provided 20% excess of the amount of CaO needed for complete removal of all CO_2. 10 mol of recycled CO_2 were fed to the regeneration reactor where 0.91 mols of additional CO_2 were formed by $CaCO_3$ decomposition. The CO_2 was then cooled and split with 0.91 mol available for compression and sequestration, and 10 mols recycled and reheated by combustion of supplemental CH_4 and 10% excess air in an indirect fired furnace.

A summary of key simulation results is presented in Table 1. In each case the 95+% H_2 product objective was achieved. The advantages of the single-step process include process simplification, elimination of shift catalysts, reduced supplemental energy, and reduced CO_2 emissions. Disadvantages include the slightly lower H_2 content of the product and the higher operating temperature of the regenerator.

Table 1. Process Simulation Comparison

Process	Conventional	Acceptor, No CO_2 Control	Acceptor, With CO_2 Control
Temp., °C	Reformer 850	Primary Reactor 650 Regenerator 972	Primary Reactor 650 Regenerator 972
Press., atm	15	15	3
Process Feed, mol			
CH_4	1	1	1
H_2O	4	4	4
Fuel CH_4, mol	0.51	0.39	0.53
Major Process Vessels	5 Reformer H.T. Shift L.T. Shift CO_2 Scrubber CO_2 Stripper	2 Primary Reactor Regenerator	3 Primary Rector Regenerator CO_2 Reheat Furnace
Shift Catalysts	2	0	0
H_2 Purity, mol%	97.9	96.5	97.7
H_2 Production Rate, mol H_2/mol CH_4	3.72	3.36	3.79
CO_2 Emission Rate, mol	1.51	1.39	0.62

EXPERIMENTAL APPARATUS AND MATERIALS

The experimental program was divided into two phases. The first phase used high purity $CaCO_3$ as the acceptor precursor and was designed to prove that the combined reaction equilibrium could be closely approached at reaction conditions of practical interest. Commercial dolomite was used as the acceptor precursor in the second phase and multicycle experimental tests were carried out to obtain preliminary information on acceptor and catalyst durability.

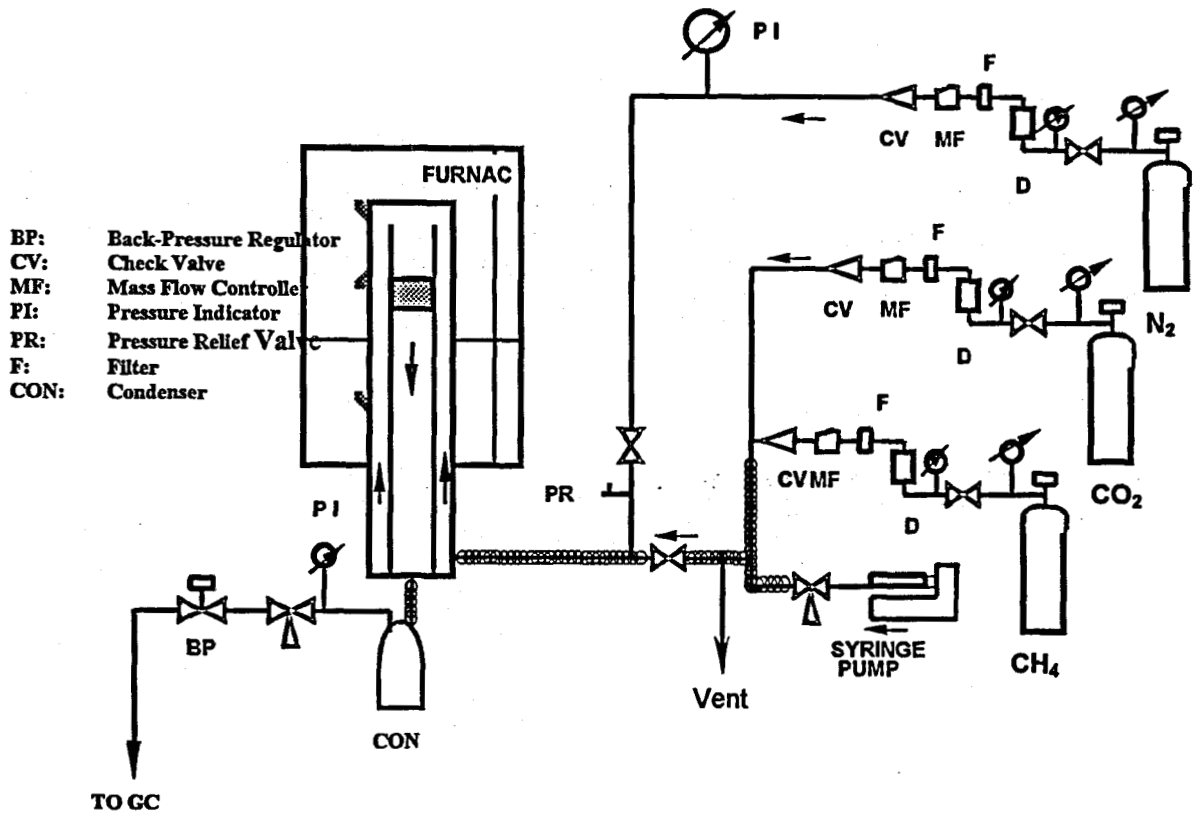

Figure 6. The Laboratory-Scale Fixed-Bed Reactor System

The laboratory-scale, fixed-bed reactor system shown in Figure 6 was used in both experimental phases. Gases were obtained from high-purity cylinders and flow rates were controlled using mass flow controllers. In those regeneration tests using air, an air cylinder was substituted for the CO_2 cylinder. Water was fed as a liquid using a high-pressure syringe pump and all lines were heat traced to insure complete vaporization. Combined feed gases entered near the bottom of the reactor and were preheated as they flowed upward in the annular area between the reactor insert and pressure vessel. The preheated gas flowed downward through a mixture of reforming catalyst and Ca-based CO_2 acceptor and exited from the bottom of the reactor. After excess steam was removed in the condenser, the pressure was reduced to 1 atm using the backpressure regulator.

Product gas was analyzed using a Shimadzu GC14A gas chromatograph equipped with an automatic 10-port sampling valve, dual columns, flame ionization and thermal conductivity detectors, and a nickel-catalyzed methanator. Traces of moisture that escaped the condenser were captured on a HayeSep N column that did not retain permanent gases. Water was backflushed from the HayeSep N column while separation occurred in a Carboxen 1000 column. Nitrogen was used as the carrier and backflush gas. Product gases eluted from the Carboxen 1000 column passed, in turn, through the thermal conductivity detector, the methanator, and the flame ionization detector. The

thermal conductivity detector was used for the analysis of H_2, CO_2 and large concentrations of CH_4; the flame ionization detector was used for CO and small concentrations of CH_4. The carbon and hydrogen material balance closure from the raw chromatograph data, which were generally within ±5%, were normalized to close the material balances and all compositions reported are based on normalized results.

The reactor packing consisted of a mixture of commercial reforming catalyst from United Catalysts, Inc. and a Ca-based acceptor. Properties of the catalyst and acceptor are summarized in Table 2. The Ni-based reforming catalyst, designation C11-9-02 was used throughout the experimental program. During Phase I a high-purity $CaCO_3$ from Mallinckrodt was used as the acceptor precursor in order to avoid complications from trace impurities. Commercial operation will require a low-cost acceptor and two inexpensive, commercial dolomites were used as acceptor precursors during Phase II. The catalyst was received in the form of rings that were crushed and sieved prior to use. Particles <150 μm were used during Phase 1 while two particle sizes, 75 – 150 μm and 300 – 425 μm, were used in Phase 2. The high-purity $CaCO_3$, with particle sizes <150 μm, was used without sieving. Two particle sizes of dolomite, 75 – 150 μm and 300 – 425 μm, were used during Phase II. Large catalyst particles were always used with small acceptor particles, or vice versa, during Phase II so that catalyst and acceptor could be separated prior to acceptor regeneration when desired.

During Phase I $CaCO_3$ was precalcined in a quartz boat in a tube furnace at 750°C and 1 atm under N_2 for 4 hours before being mixed with the catalyst and added to the reactor. Both dolomites used in Phase II had to be pretreated for sulfur removal prior to use. Without pretreatment the sulfur was transferred from the solid to the gas phase during a run and subsequently poisoned the Ni reforming catalyst. The reactor response with and without dolomite pretreatment is compared in a subsequent section of this report. Sulfur, present initially as sulfate, was first reduced to sulfide by exposure to 40%H_2/N_2 at 900°C for 6 hours. The sulfide was then removed from the solid by reaction with 40%H_2O/N_2 at 900°C for another 6 hours. The following desulfurization reactions occur.

$$CaSO_4/MgSO_4(s) + 8H_2(g) \leftrightarrow CaS/MgS(s) + 8H_2O(g) \qquad (7)$$

$$CaS/MgS(s) + 2H_2O(g) \leftrightarrow CaO/MgO(s) + 2H_2S(g) \qquad (8)$$

No problems with sulfur poisoning were found after this pretreatment procedure was implemented. The catalyst was used without pretreatment, and reduction of NiO to active Ni occurred during the initial stage of each reaction test cycle.

Catalyst and pretreated (or calcined) acceptor were physically mixed in a mass ratio of about 1:1 in Phase I and 1:3 in Phase II prior to being added to the reactor. The capacity of the reactor insert, about 14g during Phase I, was enlarged to a capacity of about 30 g for the Phase II tests. Different particle size ranges of catalyst and acceptor were used in multicycle tests to enable separation between cycles, when desired.

Table 2. Selected Properties of the Reforming Catalyst and Acceptor Precursors Used in the Experimental Program

REFORMING CATALYST (Phases I and II)

Source/Designation	United Catalysts, Inc. / C11-9-02
Chemical Composition, wt %	
Ni	12 ± 1.5
Al_2O_3	80 – 86
SiO_2	< 0.05
Sulfur	< 0.05
LOI to Constant Weight at 1000°F	< 1.0
Physical Properties	
Bulk Density, lb/ft^3	80 ± 5
Surface Area, m^2/g	3 – 10
Pore Volume, cm^3/g (> 29.2 Å)	0.10-0.20

ACCEPTOR PRECURSORS

	Phase I	Phase II	
Source	Mallinckrodt $CaCO_3$ (4071-02)	Stonelite Dolomite	Rockwell Dolomite
Chemical Composition, wt %			
$CaCO_3$	99.97	54.23	53.78
$MgCO_3$	------	44.80	45.89
Sulfur	< 0.0005	0.011	0.010
Bulk Density, lb/ft^3	------	68.2	68.2

The reactor response during a typical reaction test is shown in Figure 7. While this test is from Phase II, the responses during both phases were qualitatively the same. The feed gas in this example contained 12% CH_4, 48% H_2O, and 40% N_2 at a rate of 500cm^3(stp)/min. N_2 was used as a diluent in most tests in order to simplify system operation; however, we have shown that the composition of the reactor product on a N_2-free basis was the same as would be achieved with no diluent. Reaction conditions were 650°C and 15 atm. Other reaction parameters are listed on the figure. The dry basis composition of the reactor product as a function of time is shown by the discrete points while horizontal lines represent equilibrium compositions calculated by HSC Chemistry.

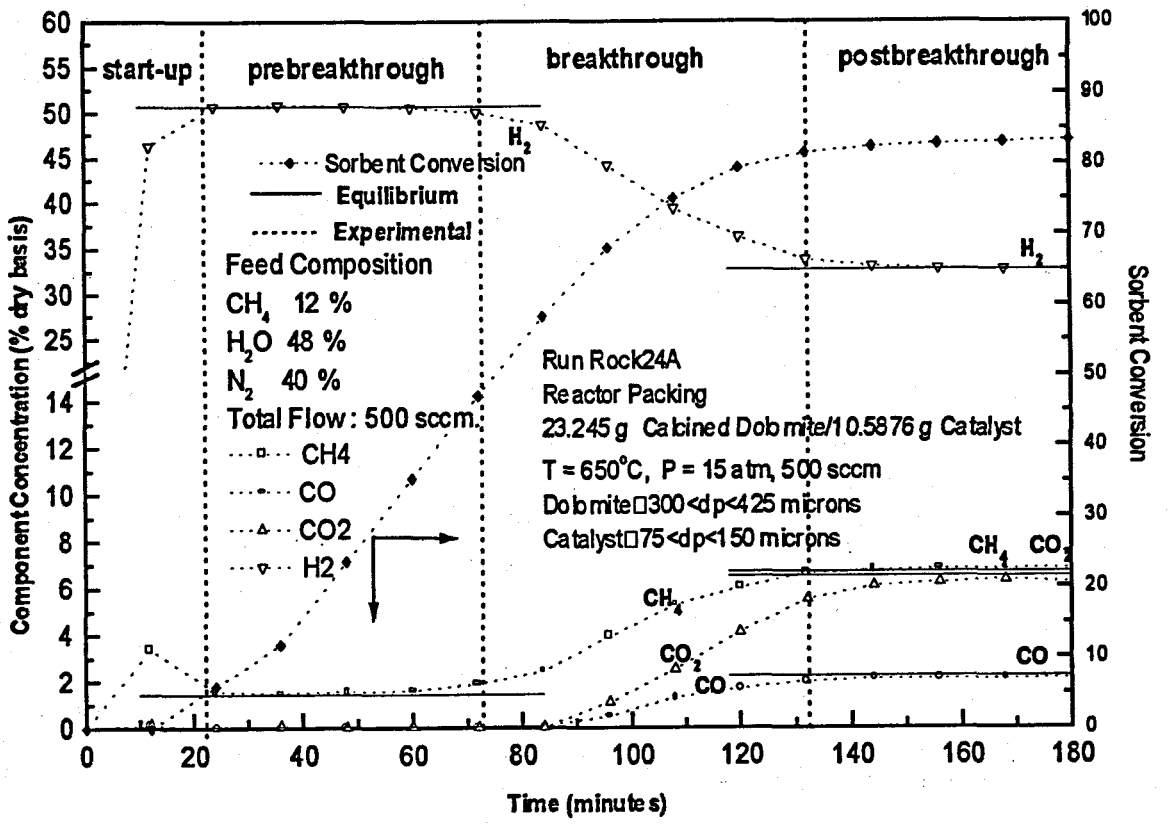

Figure 7. Reactor Response from a Typical Run.

Figure 7 is divided into 4 regions indicated by the vertical dashed lines. The first region, designated start-up, is caused by two factors. The first is associated with a time delay between opening the valve to feed gases to the reactor and those gases reaching the chromatograph sampling valve. In addition, the catalyst was added to the reactor in the inactive NiO form and time was required to reduce to NiO to active Ni. In the second region, designated prebreakthrough, the combined reforming, shift, and carbonation reactions were fully active. H_2 content was maximum and CH_4, CO, and CO_2 concentrations were minimum. Simultaneous reaction equilibrium was closely approached and all experimental concentrations were near the respective equilibrium values. For example, the experimental H_2 content of 50.9% was only marginally less than the 51.0% equilibrium value. During this period the fractional conversion of CH_4 was 0.89 and the H_2 production rate was 3.57 mol per mol of CH_4 fed. The third region, breakthrough, began after 72 minutes when the CaO-CO_2 reaction front reached the exit of the fixed bed. CO_2 removal began to decrease, which caused the CO and CH_4 concentrations to increase and the H_2 concentration to decrease. The slope of the H_2-time curve during breakthrough is a measure of the global rate of the combined reactions. During the fourth period, designated postbreakthrough, CO_2 removal was negligible, and only the reforming and shift reactions were active. Product concentrations during this period were also quite close to the combined reforming and shift equilibrium values, again designated by the horizontal solid lines. The prebreakthrough H_2 concentration of 50.9% was 56% greater than the 32.7% H_2 concentration during postbreakthrough, and the increase is directly attributable to the CO_2 acceptor.

Fractional sorbent conversion as a function of time is also shown in Figure 7. Sorbent conversion was calculated by material balance using the known quantity of CaO charged to the reactor, the feed rate of CH_4 and the total flow rate of CH_4, CO, and CO_2 in the reactor product. In this example the fractional sorbent conversion was 0.47 at the beginning of breakthrough, 0.81 at the end of breakthrough, and 0.83 when the test was terminated after 180 minutes.

Figure 8 illustrates the need for dolomite pretreatment by comparing the H_2 content as a function of time using acceptor precursor with and without pretreatment. Feed gas consisted of 6% CH_4, 24% H_2O, balance N_2 at a flow rate of 500 cm^3(stp)/min at 650°C and 15 atm. Without pretreatment, the H_2 content of the product gas increased initially but peaked at about 22% after 35 min and decreased continually for the remainder of the test. No steady-state period was reached and both the maximum and final H_2 concentrations were below the equilibrium values. The experimental H_2-time response following pretreatment was as expected. The H_2 concentration reached a prebreakthrough steady state of about 24.5%, consistent with the equilibrium value designated by the horizontal line, and remained at that level for about 200 minutes. Thereafter, the H_2 concentration decreased to a second steady state of about 16% and remained at that level until the test was terminated. The second steady state was consistent with the combined reforming and shift equilibrium, again designated by the horizontal line. Note that the duration of the prebreakthrough period is a function of the CaO charge and the flow rate and CH_4 concentration of the feed gas. No pretreatment was necessary in the Phase 1 tests using high-purity $CaCO_3$; all response curves were qualitatively similar to the Figure 8 curve corresponding to dolomite pretreatment.

H_2 concentration during the prebreakthrough and postbreakthrough periods were of maximum interest and most of the experimental results in the following sections are based on these values rather than the entire breakthrough curves.

PHASE I EXPERIMENTAL RESULTS

All Phase I tests were limited to a single reaction cycle and were designed to prove the feasibility of the single-step H_2 process and to obtain performance data over a range of reaction conditions. All tests were conducted at 15 atm while temperature and the composition and flow rate of the feed gas served as reaction parameters.

The effect of temperature on H_2 concentration during the prebreakthrough and postbreakthrough periods is shown in Figure 9. Reactor feed contained 6% CH_4, 24% H_20 and 70% N_2 at a rate of 500cm^3(stp)/min and the temperature was varied between 450°C and 750°C. Equilibrium lines corresponding combined reforming, shift, and carbonation (prebreakthrough) and to combined reforming and shift (postbreakthrough) are shown for comparison. Experimental results are represented by discrete points.

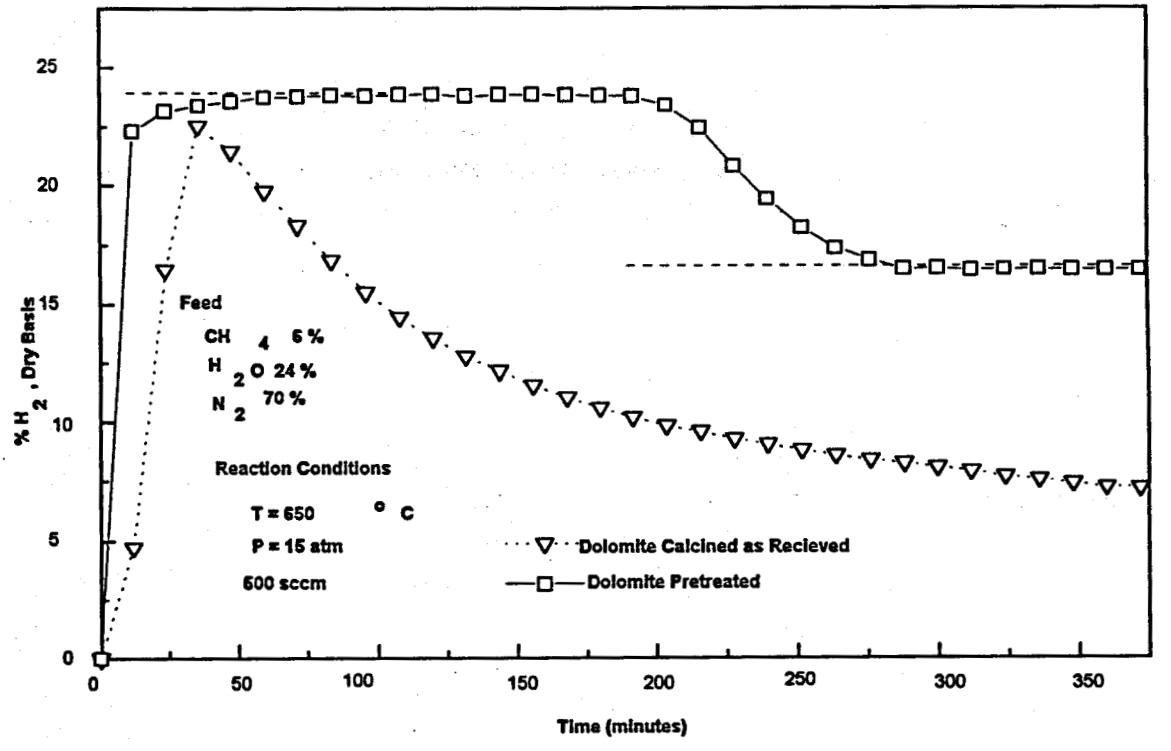

Figure 8. Reactor Response With and Without Dolomite Pretreatment

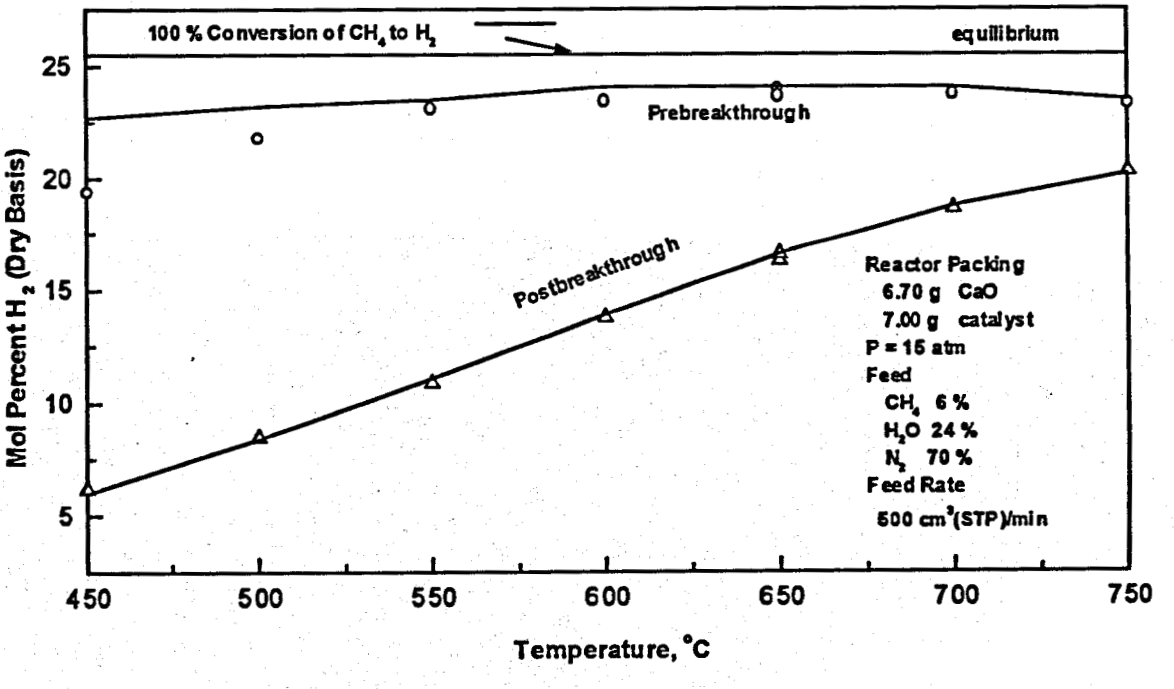

Figure 9. Hydrogen Content as a Function of Temperature.

Prebreakthrough equilibrium is based on $Ca(OH)_2$-free calculations. Key features of this figure include (1) the close approach of the experimental and equilibrium values in both the prebreakthrough and postbreakthrough periods, (2) the relative independence of the experimental prebreakthrough H_2 content to temperature above 550°C, and (3) the large increase in the H_2 content in the prebreakthrough period compared to the postbreakthrough period, particularly at lower temperatures.

All prebreakthrough and postbreakthrough H_2 concentrations are within one percentage point of the corresponding equilibrium values except at 450°C and 500°C. Between 550°C and 750°C the experimental prebreakthrough H_2 concentrations varied only between 23.1% and 23.9%, while equilibrium values over this temperature range varied between 23.2% and 24.1%. This lack of temperature dependence is a result of the combined reactions being approximately thermally neutral. From a practical standpoint the lack of temperature dependence means that a commercial process could experience reasonably wide temperature variations with little effect on product H_2 concentration. In contrast, H_2 concentration during postbreakthrough was strongly temperature dependent with experimental values increasing from 6.2% at 450°C to 20.3% at 750°C, consistent with the endothermic nature of the reforming reaction and illustrating the need to operate the conventional reformer at high temperature. At still higher temperatures where $CaCO_3$ can no longer be formed there would be no difference in prebreakthrough and postbreakthrough performance. The reproducibility of experimental results at equivalent reaction conditions was quite good as shown by the results of duplicate tests at 650°C. Prebreakthrough H_2 concentrations of 23.9% and 23.8% and postbreakthrough concentrations of 16.6% and 16.5% were measured in the two tests. The experimental prebreakthrough concentrations at 450°C and 500°C were considerably below equilibrium, which may have been caused by formation of $Ca(OH)_2$ or by slower carbonation kinetics or a combination of both.

Varying the steam-to-methane feed ratio while keeping the CH_4 concentration constant produced the results shown in Figure 10. Fractional conversion of CH_4 during the prebreakthrough and postbreakthrough periods is plotted versus steam-to-methane ratio. Reaction conditions were 650°C and 15 atm. Increasing the ratio from 3 to 5 increased the prebreakthrough fractional CH_4 conversion by 11%, from 0.87 to 0.97. The postbreakthrough CH_4 conversion increased by 17%, from 0.64 to 0.75. The 11% increase in H_2 conversion during prebreakthrough produced a 19% increase in H_2 production rate while the 17% increase during postbreakthrough produced a 24% increase in H_2 production rate.

All experimental tests shown in Figures 9 and 10 used approximately equal quantities of reforming catalyst and CaO. In order to increase the CH_4 concentration of the feed gas and/or the feed gas flow rate, larger quantities of CaO were needed so that sufficient data could be collected to properly define the breakthrough curves. The ratio of CaO to catalyst was increased by successively reducing the amount of catalyst from 7g to 5g and to 3g, while increasing the amount of acceptor from 7g to 9g to 10g. Different bed densities associated with the two solids made strictly proportional changes impossible. The reduced quantity of catalyst was still sufficient to permit both

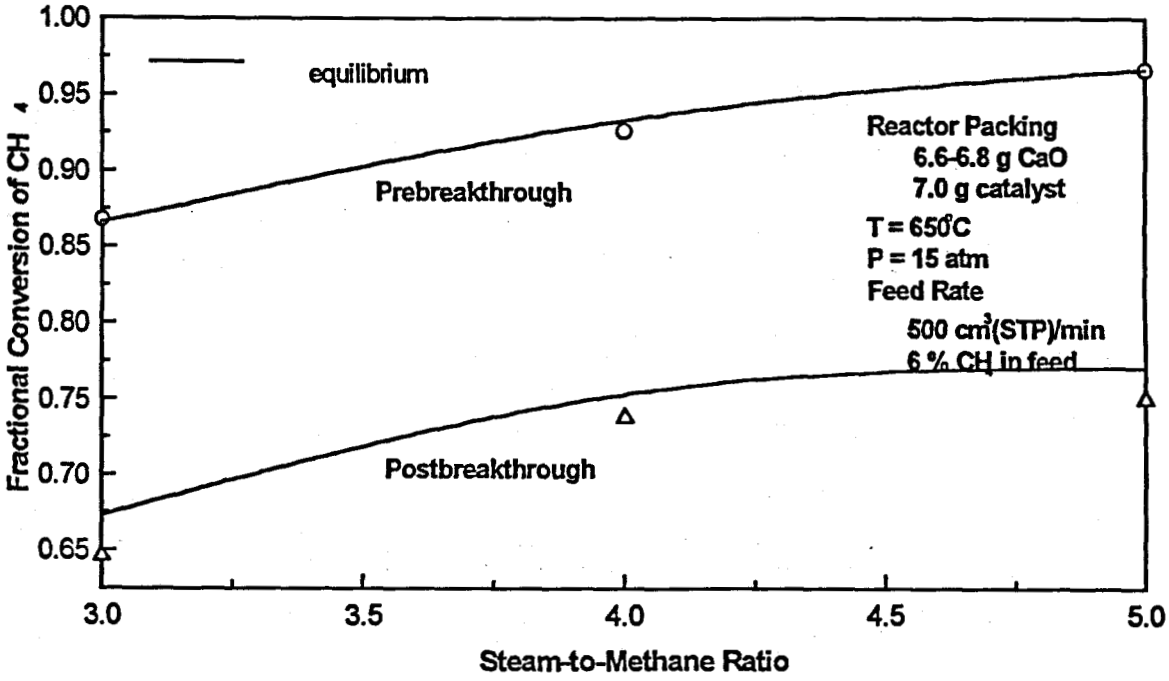

Figure 10. CH_4 Fractional Conversion as a Function of Steam-To-Methane Ratio

prebreakthrough and postbreakthrough equilibrium to be closely approached while the increased quantity of acceptor extended the duration of the prebreakthrough period by about one-third and provided the flexibility needed to increase the CH_4 content and/or the feed gas rate.

With the increased acceptor loading it was possible to collect sufficient experimental data during a test to permit the volumetric feed rate to be increased. The feed rate using 6% CH_4 and steam-to-methane ratio of 4 at 650°C and 15 atm was varied between 250cm^3(stp)/min and 1200cm^3(stp)/min with prebreakthrough and postbreakthrough H_2 concentrations shown in Figure 11. Increasing the volumetric feed rate reduced the duration of the prebreakthrough period but had little effect on product gas H_2 concentration. During prebreakthrough the experimental H_2 concentration ranged from 23.6% to 24.2% compared to 24.1% at equilibrium. Postbreakthrough H_2 concentrations ranged from 15.6% to 17.0% compared to the equilibrium value of 16.7%. The reaction rates were sufficiently large that equilibrium was closely approached, except for a small drop off at 1200cm^3(stp)/min. The good reproducibility is again evident in Figure 11 from results of duplicate tests at both 800cm^3(stp)/min and 1200cm^3(stp)/min.

The CH_4 concentration in the feed gas was the last reaction parameter studied in the Phase I tests. The feed gas in a commercial process contains only CH_4 and H_2O and no N_2 diluent. Consequently, the CH_4 concentration was increased incrementally from 6% to 20% at a constant H_2O-to-CH_4 ratio of 4. N_2 diluent was incrementally decreased

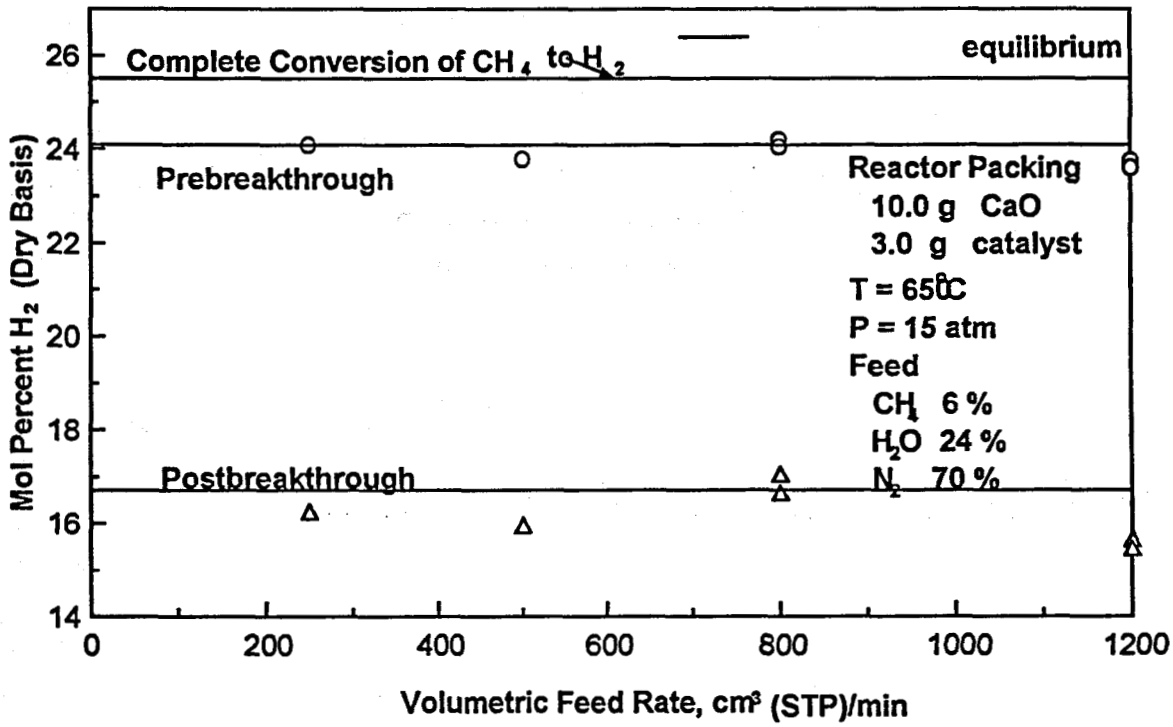

Figure 11. H_2 Concentration as a Function of Volumetric Feed Rate

and was absent in the final test where the feed gas contained 20% CH_4. 650°C and 15 atm reaction conditions were used. The feed rate was gradually reduced from 500cm^3(stp)/min, and was only 200cm^3(stp)/min when the feed contained 20% CH_4. Again, the reduced feed rate was necessary to extend the duration of the run to permit sufficient data to be collected to properly characterize the breakthrough curve.

Prebreakthrough and postbreakthrough H_2 concentrations as a function of the CH_4 concentration of the feed are shown in Figure 12 along with the corresponding equilibrium values. Once again the experimental and equilibrium values were quite close, and the H_2 concentration during prebreakthrough was roughly 50% greater than the corresponding postbreakthrough value. The experimental H_2 concentration using 20% CH_4 was 94.7%, compared to 96.1% at equilibrium.

PHASE II EXPERIMENTAL RESULTS

Single Reaction Cycle

Two commercial dolomites whose properties were summarized in Table 2 were used as acceptor precursors during the Phase II tests in place of the high purity $CaCO_3$ used in Phase I. Dolomite was chosen over limestone even though it has a lower CO_2 capacity because earlier tests in this laboratory (Silaban et al. 1996) showed improved

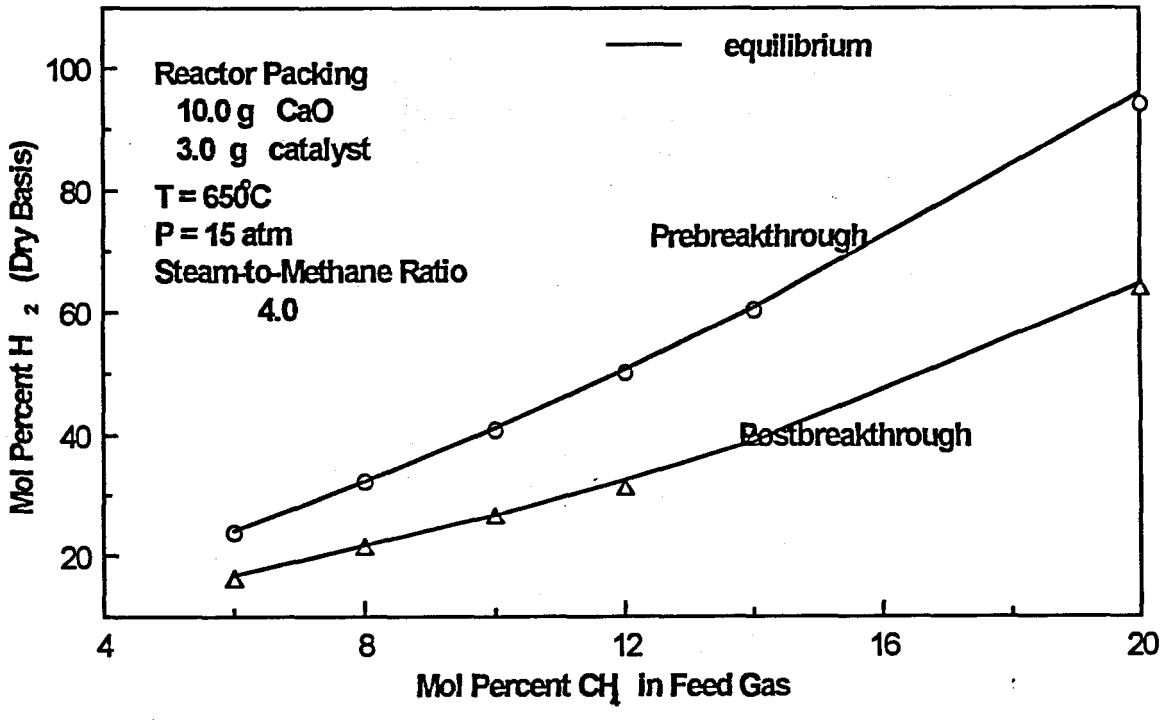

Figure 12. Product H_2 Concentration as a Function of Feed CH_4 Concentration

multicycle durability. The need to pretreat the dolomite to remove sulfur and prevent poisoning of the Ni reforming catalyst has been discussed previously.

A limited number of single-cycle reaction tests were conducted to confirm that results using pretreated dolomite were comparable to those using the high purity $CaCO_3$. The time response from one such run using a feed composition of 20% CH_4 and 80% H_2O (no N_2 diluent) at a rate of 200cm^3(stp)/min is shown in Figure 13. Reaction conditions were 650°C and 15 atm; the fixed bed contained 29.5g of calcined Rockwell dolomite and 10.9g of standard reforming catalyst. The four regions of the reactor response curve are clearly visible, and H_2, CH_4, CO, and CO_2 concentrations are near their respective equilibrium values during both the prebreakthrough and postbreakthrough periods. The relatively short duration of the prebreakthrough period is due to the large CH_4 feed rate. Maximum prebreakthrough H_2 concentration was 95.8% compared to 96.1% at equilibrium. Fractional calcium conversion, again calculated by material balance, was 0.71 at the beginning of breakthrough and 0.90 at the end of breakthrough.

The effect of temperature using Rockwell dolomite is illustrated in Figure 14 where results from single-cycle runs at 650°C and 550°C are compared. Feed gas for these two tests contained 16% CH_4, 64%H_2O, and 20% N_2 diluent. Prebreakthrough H_2 concentration at 650°C was 71.6%, only 0.2% below equilibrium, compared to 66.6% at

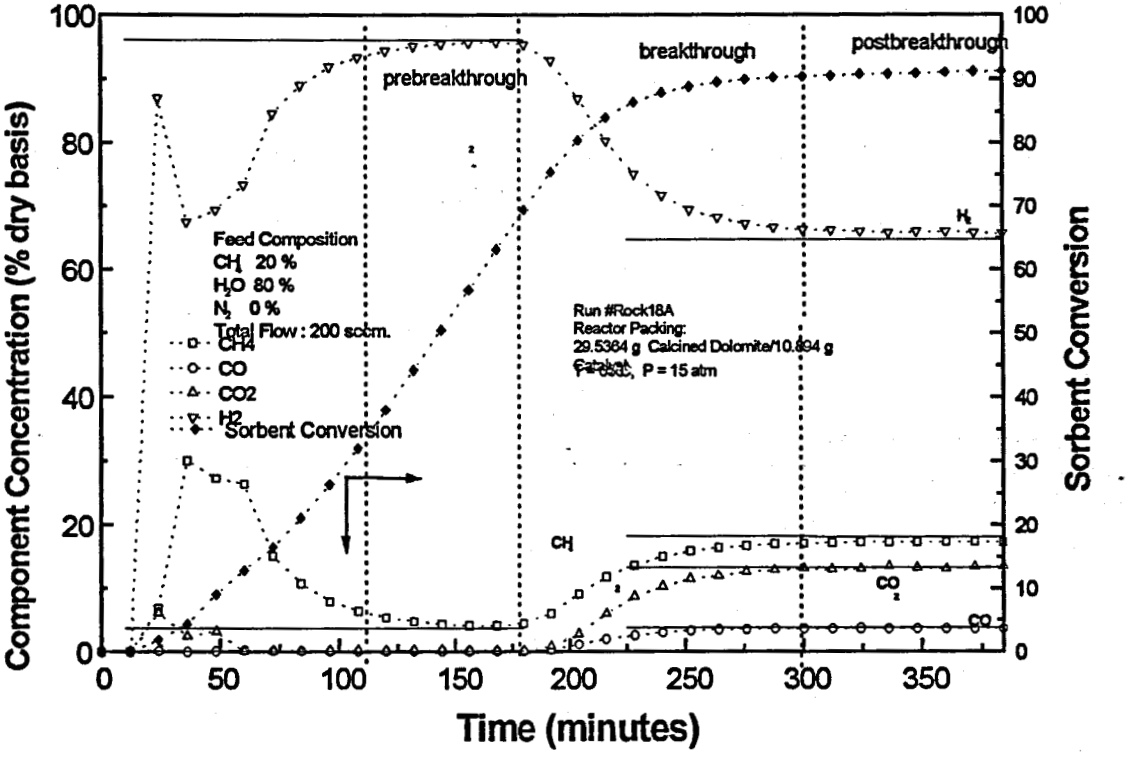

Figure 13. Single-Cycle Run Using Dolomite Acceptor and Showing the Production of 95+% H_2.

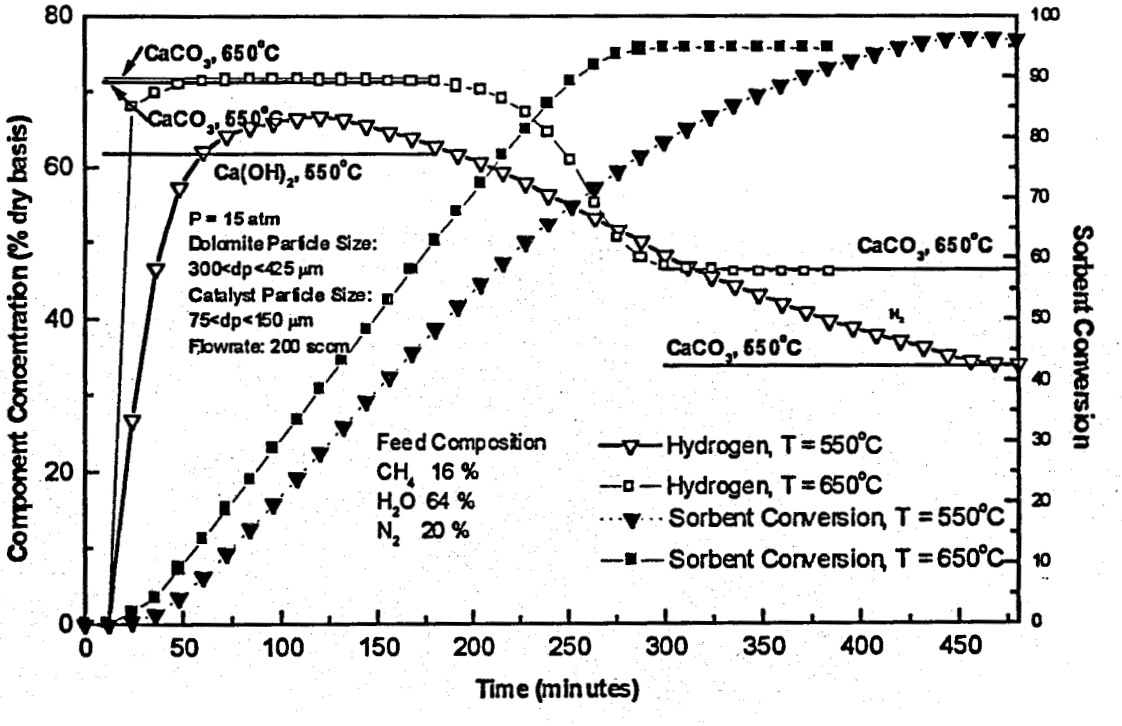

Figure 14. Reactor Response at 550°C and 650°C Using Dolomite Acceptor

550°C. The 550°C experimental value was between the equilibrium values corresponding to $CaCO_3$ only (71.3%) and both $CaCO_3$ and $Ca(OH)_2$ (61.8%). The slope of the breakthrough curve was also much smaller at 550°C. Final fractional calcium conversion was about 0.95 in both tests even though a longer time was required to reach the final conversion at 550°C. The lower maximum prebreakthrough concentration could be due to slower kinetics or to the formation of $Ca(OH)_2$ or both. While the reduced slope of the breakthrough curve at 550°C is a definite indication of reduced global kinetics, the fact that the postbreakthrough H_2 concentration at 550°C reached the equilibrium level after about 450 min shows that the reforming catalyst was still highly active.

When equivalent particle size ranges and pretreatment conditions were employed there was little, if any, difference in system performance using Rockwell and Stonelite dolomite. In two runs using large acceptor particles (300 μm < d_p < 425 μm) and small catalyst particles (75 μm < d_p < 150μm), prebreakthrough and postbreakthrough equilibrium were closely approached with each acceptor and the slopes of the breakthrough curves were similar. Fractional calcium conversions at the beginning of breakthrough were 0.74 in both cases, and the final calcium conversion was 0.86 for Stonelite dolomite and 0.85 for Rockwell.

The final reaction parameter studied in the single cycle tests was particle size. Reaction conditions were 650°C and 15 atm using 500cm^3(stp)/min of feed gas containing 12% CH_4, 48% H_2O, and 40% N_2. In one test large Rockwell dolomite particles (300 μm < d_p < 425 μm) were combined with small catalyst particles (75 μm < d_p < 150 μm), and the particles sizes were reversed in the second test. Reactor response curves are shown in Figure 15. Once again, prebreakthrough and postbreakthrough H_2 concentrations closely approached equilibrium values in both tests, and final fractional sorbent conversions were approximately equal. There was, however, a significant difference in the slopes of the breakthrough curves, with the slope being much smaller with the larger acceptor particles. Since the slope of the breakthrough curve is a measure of the global reaction rate, these results are consistent with the rate of CO_2 removal being influenced by transport resistances within the larger acceptor particles.

Multiple Reaction-Regeneration Cycles

Having shown that pretreated commercial dolomite was a satisfactory CO_2 acceptor, additional experimental tests were conducted to provide preliminary information on the multicycle durability of the catalyst-acceptor mixture as a function of regeneration conditions. Standard conditions were chosen for the reaction portion of each cycle while temperature and gas composition were the regeneration parameters studied (see Table 3). In some multicycle tests the catalyst and spent acceptor were cooled and separated by sieving before the acceptor was regenerated. The catalyst and regenerated acceptor were then mixed once again and added to the reactor for the subsequent reaction cycle. This procedure, however, was very time consuming and only a limited number of such tests were completed. In addition, some catalyst and acceptor were invariably lost during sieving, and variations in solids mixing may have affected

subsequent cycle reaction performance. The effect of regeneration conditions was evaluated by comparing the performance in the subsequent reaction cycles.

All regeneration tests were limited to 1 atm because of safety considerations associated with the reactor system at the higher regeneration temperatures. A minimum regeneration temperature of 800°C is needed to achieve acceptably fast regeneration kinetics while the maximum temperature of 950°C was selected because it is near the temperature required for regeneration in pure CO_2 at 1 atm.

The regeneration gas compositions were chosen to simulate possible regeneration modes, with 100% N_2 used as reference. Heating the acceptor from reaction to regeneration temperature via direct combustion of supplemental fuel with 10% excess air will produce an atmosphere composed primarily of N_2 with about 4% O_2. This composition is of particular importance if the reforming catalyst remains in contact with the acceptor during regeneration. Oxidation of active Ni to NiO would occur in each regeneration cycle and the catalyst would have to be re-reduced at the beginning of each reaction cycle. Production of a pure CO_2 off-gas for greenhouse gas control as described in the process simulation section will require that the regeneration atmosphere be pure CO_2. If the catalyst remains in contact with the acceptor in this case, it would be exposed to the higher regeneration temperature but would remain in the active reduced state. In the following discussion the term *in situ* is used to describe tests in which the acceptor and catalyst were not separated between cycles, i. e., both were exposed to regeneration conditons.

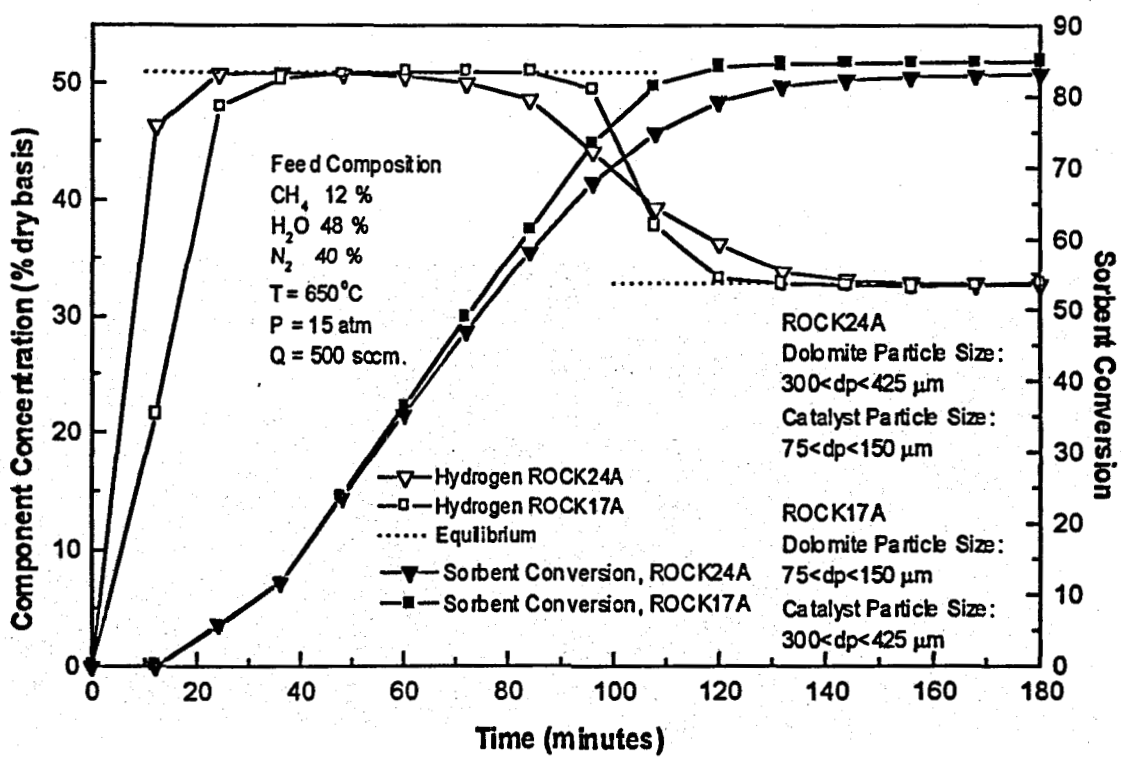

Figure 15. Acceptor Particle Size Effect

Table 3. Summary of Reaction and Regeneration Conditions Used in Multicycle Tests.

Reaction Phase

Pressure		15 atm
Temperature		650°C
Pretreated Acceptor-to-Catalyst Mass Ratio		2.5 – 2.7
Volumetric Feed Rate cm^3(stp)/min		500
Feed Composition, mol%		
CH_4		12
H_2O		48
N_2		40
Steam-to-Carbon Molar Ratio		4

Regeneration Phase

Pressure		1 atm
Temperature		800°C – 950°C
Gas Composition	(1)	100% N_2
	(2)	4%O_2/96%N_2
	(3)	100%CO_2
Catalyst	(1)	Separated from acceptor
	(2)	In contact with acceptor

Multicycle research began with a series of five-cycle tests which examined the effects of regeneration temperature, atmosphere, and catalyst-acceptor contact during regeneration. Five-cycle results using Rockwell dolomite and "mild" *in situ* regeneration conditions of 800°C in N_2 are shown in Figure 16. With the exception of scatter in the first sample the results were effectively identical. Prebreakthrough and postbreakthrough concentrations were equal in each cycle and also effectively equal to the equilibrium values. In addition, the slopes of the breakthrough curves were effectively identical. Similar results were obtained in a five-cycle test using Stonelite dolomite and "severe" regeneration conditions of 950°C in 4% O_2/N_2 as shown in Figure 17. There was minor scatter in these data but no obvious trends that would indicate performance deterioration. Prebreakthrough and postbreakthrough equilibria were achieved in all cycles and the slopes of the breakthrough curves were similar. In addition to the direct effect of temperature on the acceptor and catalyst, both were exposed to the different regeneration atmospheres. After the initial reduction in the first reaction cycle the catalyst remained in reduced form during N_2 regeneration, but the catalyst was oxidized and reduced in each cycle when exposed to 4% O_2.

Figure 18 shows five-cycle reaction results in a test where the catalyst and acceptor were separated prior to acceptor regeneration. Rockwell dolomite was used and

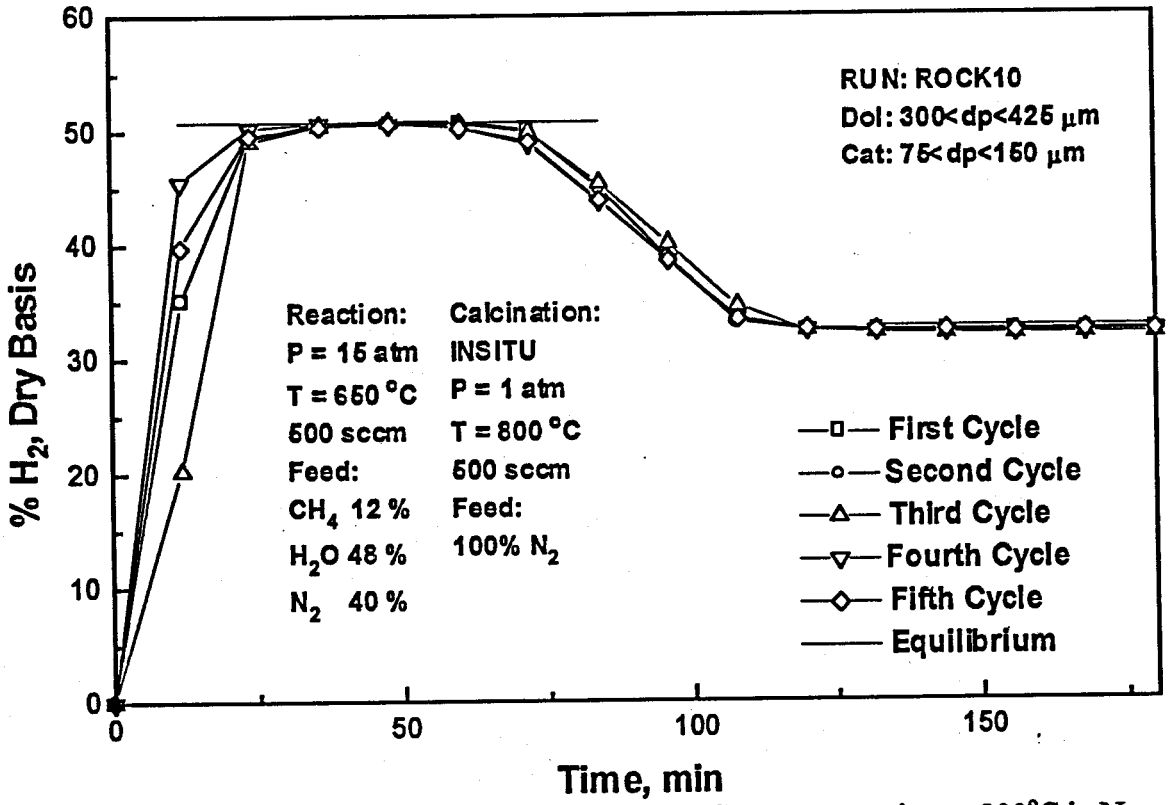

Figure 16. Five-Cycle Reaction Results Following *In Situ* Regeneration at 800°C in N_2

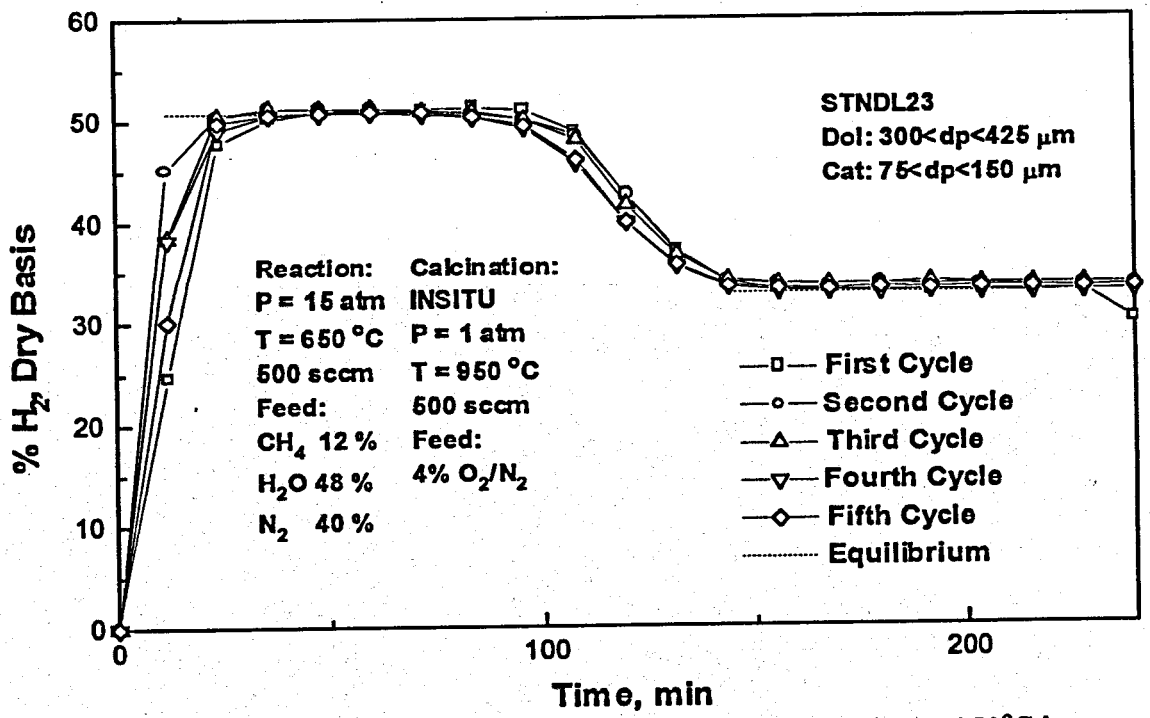

Figure 17. Five-Cycle Reaction Results Following *In Situ* Regeneration at 950°C in $4\%O_2.N_2$.

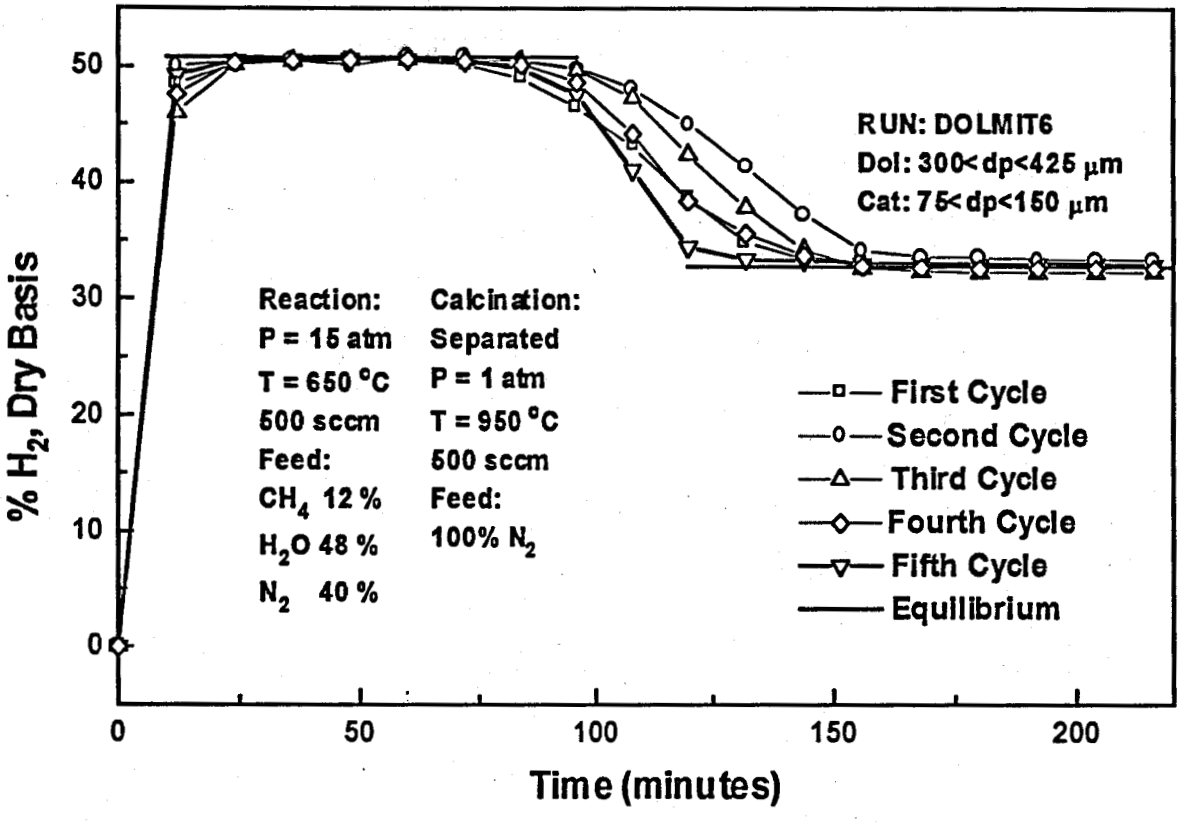

Figure 18. Five-Cycle Results Following Regeneration at 950°C in N_2 With Catalyst-Acceptor Separation

regeneration was conducted at 950°C in N_2. Surprisingly there was less data scatter during the early stages of each reaction cycle, but more scatter during the active breakthrough period. This is attributed to losses of catalyst and/or acceptor that occurred during sieving, changes in particle sizes due to attrition during sieving, and by different packing arrangements after re-mixing the solids. This scatter appeared to be reasonably random. For example, the order of breakthrough time was cycle 2 > cycle 3 > cycle 1 ~ cycle 4 > cycle 5. Performance deterioration associated with regeneration conditions should be cumulative.

A number of longer duration tests consisting of from 15 to 25 cycles completed the experimental program. No O_2 was used during these longer-duration tests because of high temperature oxidation damage to the reactor insert that was observed following the five-cycle tests. In addition, all longer duration tests used *in situ* regeneration because of the extended time required to complete a 25-cycle test with catalyst-acceptor separation between each cycle.

H_2 breakthrough curves from selected reaction cycles of a 25-cycle test following regeneration in 100% N_2 at 800°C are shown in Figure 19. H_2 concentrations during both steady-state periods were effectively equal to the equilibrium values for all 25 cycles. However, the duration of the prebreakthrough period decreased slowly beginning in cycle

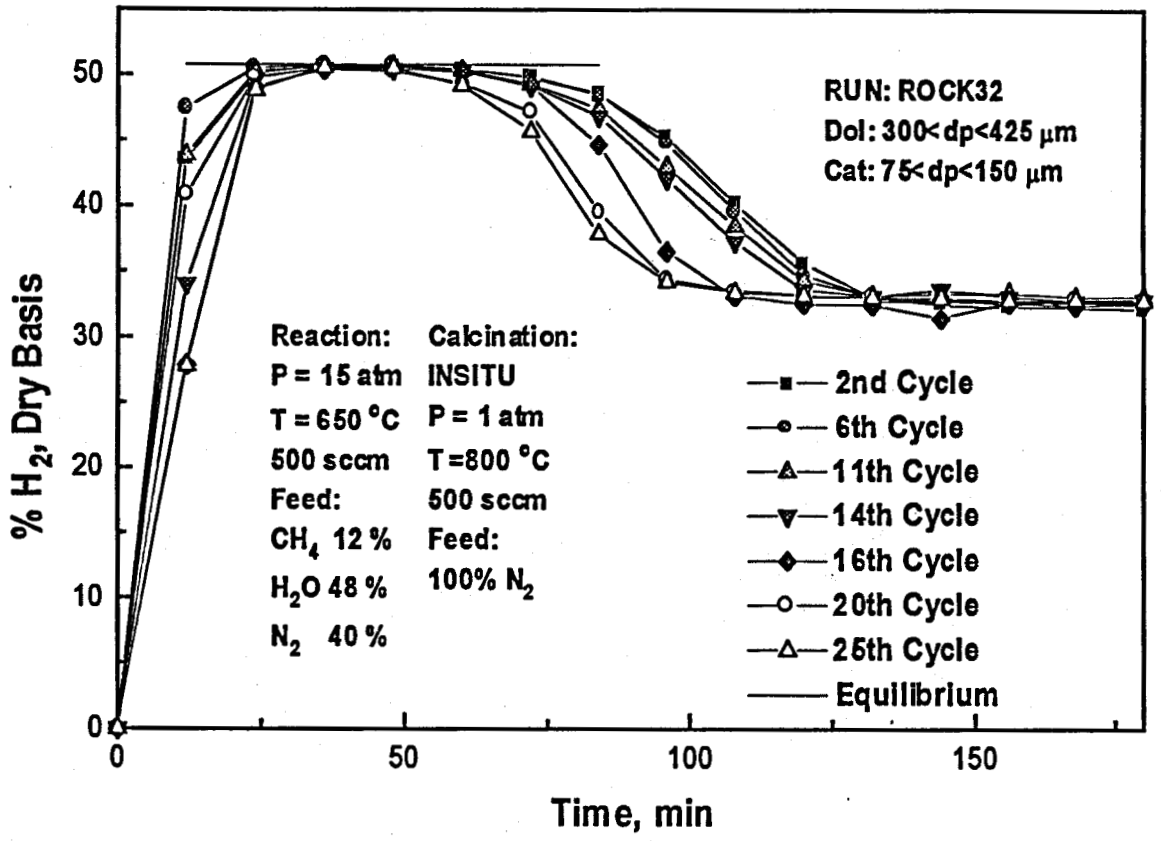

Figure 19. H_2 Breakthrough Curves from Selected Cycles of a 25-Cycle Test

7. Similar results were observed in a 25-cycle test with regeneration in N_2 at 850°C, but the rate of deterioration increased following regeneration at 950°C in N_2. In the latter case the prebreakthrough H_2 concentration was measurably less than the equilibrium value beginning in about cycle 10, and the slope of the breakthrough decreased severely. Significantly, the H_2 concentration during the postbreakthrough periods in all cycles in all tests remained very near the expected equilibrium value, which suggested that most of the deterioration was associated with the acceptor rather than the reforming catalyst.

Because breakthrough curves from longer duration tests quickly become so crowded with experimental data that it is difficult to distinguish the results, subsequent comparisons are based on the maximum H_2 concentration during prebreakthrough, breakthrough time, and fractional acceptor conversion at the beginning of breakthrough. All results are normalized to first-cycle results. Four longer-duration tests were completed, three tests using N_2 regeneration at 800°C, 850°C, and 950°C (all previously mentioned) and one test using CO_2 regeneration at 950°C.

The normalized maximum H_2 concentrations as a function of cycle number are shown in Figure 20. At 800°C in N_2 the hydrogen concentrations appear to be randomly scattered between about ±1% of the first cycle value. There is no apparent decrease in maximum H_2 with cycle number, which would indicate deterioration. The results using 850°C regeneration in N_2 were slightly more scattered, but still within about ±1.5% of the

first cycle value, and again there was no apparent decrease with cycle number. In contrast the maximum H_2 concentration following 950°C regeneration in N_2 began to decrease significantly after the fifth cycle and was only about 0.95 when that test was terminated after 15 cycles. Surprisingly, results following regeneration at 950°C in CO_2 were significantly better. Again the maximum H_2 concentration appeared to be randomly scattered with ±1% of the first cycle concentration throughout the entire 25-cycle test.

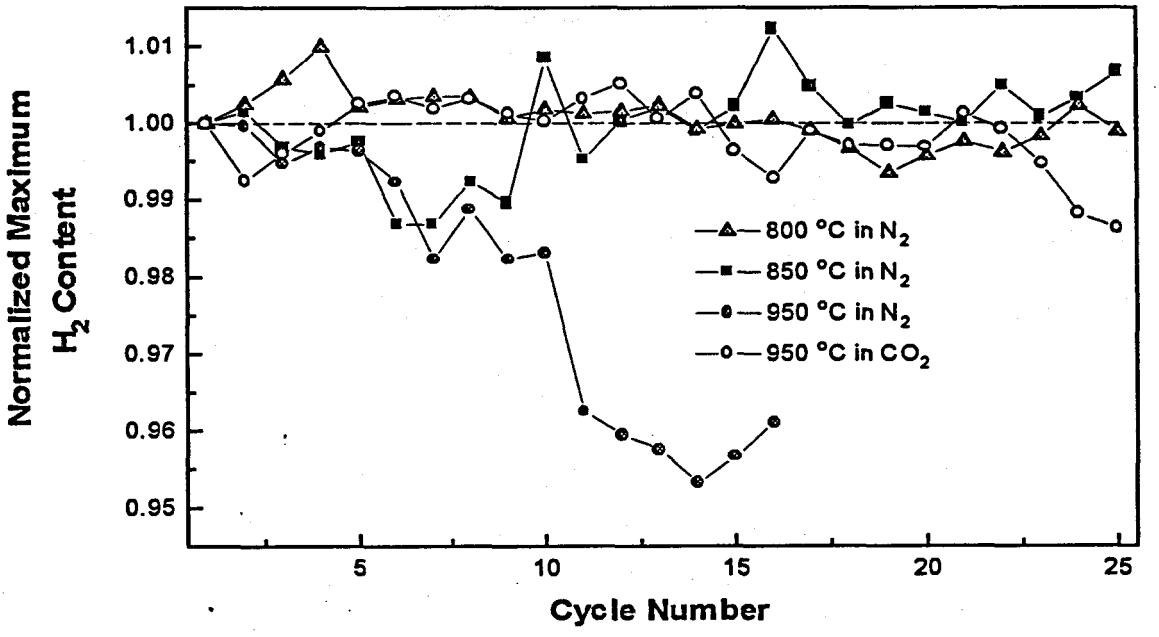

Figure 20. Normalized Maximum H_2 Concentration as a Function of Cycle Number

A similar plot showing normalized breakthrough time as a function of cycle number for the four longer-duration runs is shown in Figure 21. In this analysis, the breakthrough time was defined as the time required for the H_2 concentration to decrease from 50% to 35%, two percentage points below the prebreakthrough equilibrium value to two percentage points above the postbreakthrough equilibrium. In the few cases, limited to the last few cycles of the 950°C regeneration in N_2 test, where the maximum H_2 concentration was more than two percentage points below prebreakthrough equilibrium the beginning of breakthrough was taken to be the time when the H_2 concentration decreased by two percentage points below the maximum H_2 concentration. It is also important to note that evaluation of breakthrough time required interpolation between discrete points so that some scatter is inherent in the calculation.

There are no apparent trends in the breakthrough time except, once again, for the test in which regeneration was conducted at 950°C in N_2. The breakthrough time began to increase significantly in cycle 10 and reached a normalized value of 6 by cycle 15. In the other three longer duration tests the breakthrough time appeared to vary randomly between about ±50% of the first cycle value. Breakthrough time provides a rough measure of the global reaction rate, and a large increase in breakthrough time corresponds to a large decrease in global rate.

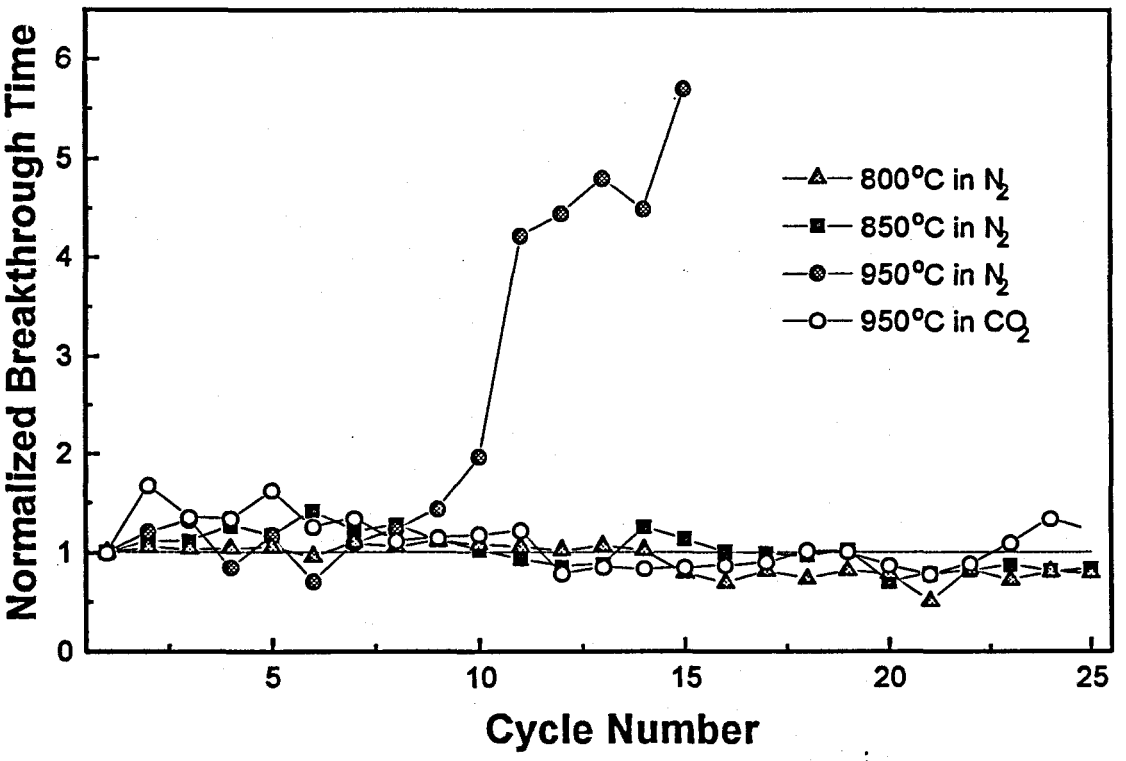

Figure 21. Normalized Breakthrough Time as a Function of Cycle Number

There are no apparent trends in the breakthrough time except, once again, for the test in which regeneration was conducted at 950°C in N_2. The breakthrough time began to increase significantly in cycle 10 and reached a normalized value of 6 by cycle 15. In the other three longer duration tests the breakthrough time appeared to vary randomly between about ±50% of the first cycle value. Breakthrough time provides a rough measure of the global reaction rate, and a large increase in breakthrough time corresponds to a large decrease in global rate.

Normalized sorbent conversion at the beginning of breakthrough decreased with increasing cycle number in all tests as shown in Figure 22. In N_2 at both 800°C and 850°C the final values were about 70% of the first cycle values, while in CO_2 at 950°C the final value was only about 30% of the first cycle value. However, much of the decrease in the CO_2 test occurred between cycles 01 and 02. Thereafter the slopes of the lines corresponding to N_2 regeneration and 800°C and 850°C and CO_2 regeneration at 950°C were approximately equal. Once again, multicycle performance deteriorated more rapidly in the 950°C in N_2 test, where the normalized sorbent conversion decreased to about 0.1 after 15 cycles.

Two longer duration dolomite calcination-carbonation tests, the first lasting 33 cycles and the second 148 cycles, were carried out using an electrobalance reactor to provide comparison with the fixed-bed multicycle test results using CO_2 regeneration. The electrobalance monitors the solid weight change associated with reaction but provides no information on product gas composition. Dolomite (no reforming catalyst) was exposed to pure CO_2 at 1 atm while the temperature was continually cycled between

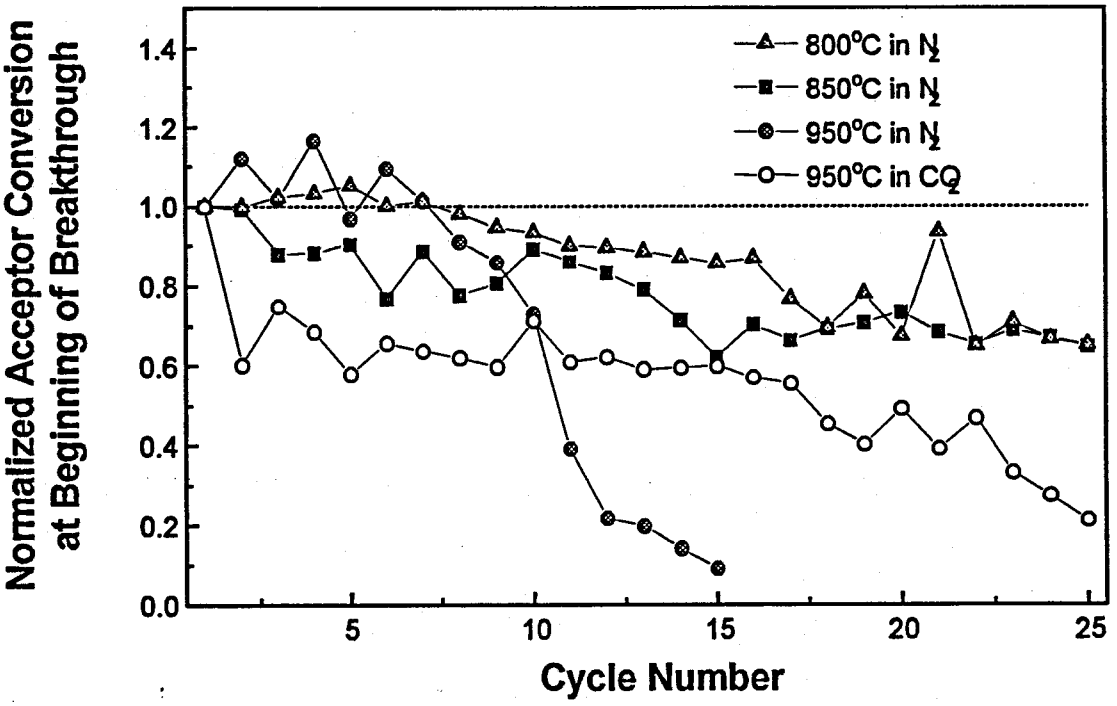

Figure 22. Normalized Sorbent Conversion at the Beginning of Breakthrough as a Function of Cycle Number.

800°C for carbonation and 950°C for calcination. The temperature was held constant for 5 min at both the maximum and minimum temperatures and was changed at a rate of 10°C/min between the temperature limits. Calcination was complete in each cycle at the end of the 950°C isothermal period but carbonation was still occurring slowly when the temperature began to increase from 800°C. Thus the electrobalance results represent the degree of carbonation achieved under the specified conditions while multicycle fixed-bed results represent the maximum achievable carbonation.

Fractional carbonation results from the two electrobalance tests are compared to similar results from the fixed-bed reactor test using 950°C regeneration in CO_2 in Figure 23. In the 33-cycle electrobalance test the fractional carbonation decreased gradually from 0.82 in cycle 01 to 0.49 in cycle 33. In the 148-cycle electrobalance test fractional carbonation decreased from 0.83 in cycle 01 to 0.26 in cycle 97. This was followed by an unexpected increase to 0.34 in cycle 104 and a second decrease to 0.27 in cycle 148. Results from the fixed-bed test were similar where the fractional carbonation decreased from 0.87 in cycle 01 to 0.52 in cycle 25. The slightly larger fractional carbonation in the early cycles of the fixed-bed test is due to the fact that these tests were carried out to completion while the electrobalance tests operated on the fixed time cycle. Nevertheless, the close similarity between fixed-bed and electrobalance reactor results also suggests that much of the decrease in multicycle activity can be attributed to the acceptor rather than the catalyst.

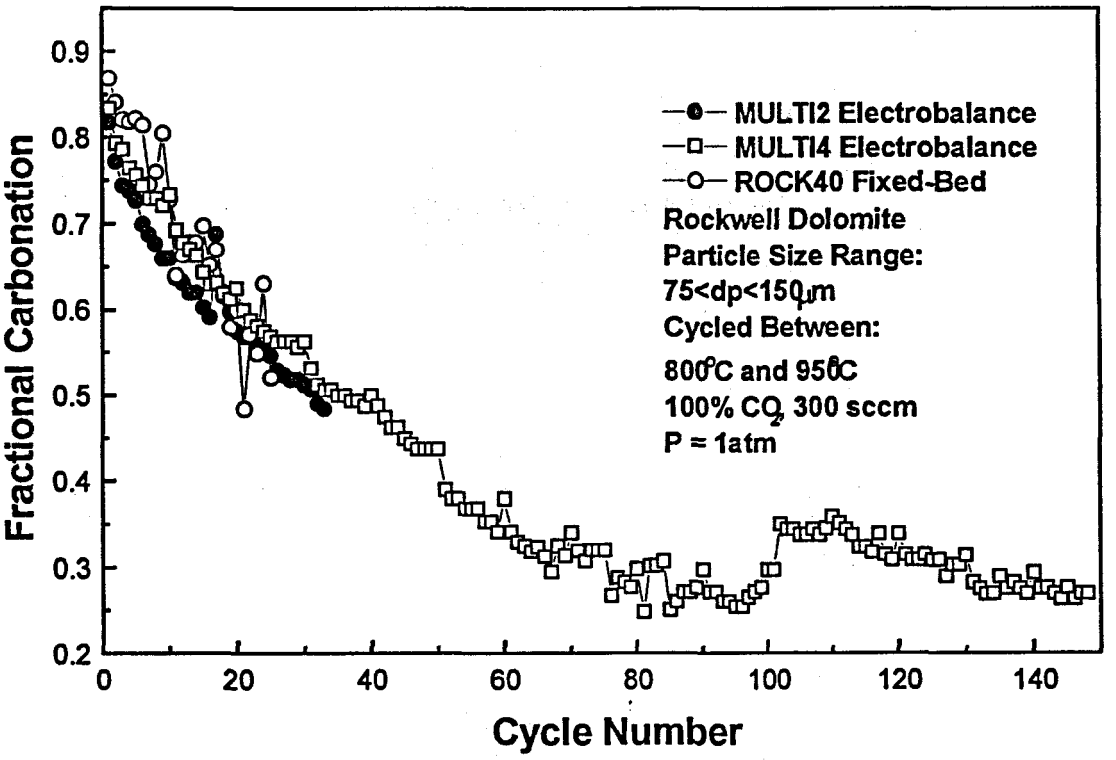

Figure 23. Comparison of Fractional Carbonation Achieved in Electrobalance and Fixed-Bed Reactor Tests.

SOLIDS CHARACTERIZATION

Limited sorbent and catalyst characterization tests were performed to supplement the reaction results. X-ray diffraction spectra of unused catalyst, both as-received and following reduction, clearly matched library spectra for NiO and Al_2O_3 and Ni and Al_2O_3, respectively. Similarly, the spectra of pretreated dolomite clearly showed that CaO and MgO were the dominant species. There was concern that mixed metal compounds that would have an adverse effect on acceptor and/or catalyst activity could be formed during the high temperature, long duration tests. For example, Alzamora et al. (1981) reported that $NiAl_2O_4$ formation might begin near 700°C with the rate of formation increasing at higher temperature. Agnelli et al. (1987) reported that $Ca_{12}Al_{14}O_{33}$ was formed when the reforming catalyst support also contained CaO. Similar compounds could be formed in this system through interaction of the Al_2O_3 catalyst support with CaO from the acceptor. However, x-ray diffraction showed no evidence of mixed metal compounds after multicycle tests, although small concentrations would not necessarily be visible in the spectra.

The activity of the reforming catalyst may also decrease due to agglomeration of nickel crystallites at high temperature. Numaguchi et al. (1995) reported that average crystallite size increased from 25nm to 40nm when the catalyst was exposed to an atmosphere of $H_2O/H_2/N_2$ for 430 hours at temperatures ranging from 590°C to 750°C.

XRD line broadening analysis using the MUDMASTER software developed by he U. S. Geological Survey (Eberl et al. 1996) was used to evaluate nickel crystallite agglomeration in this study. Texeira and Giudici (1999) also used this method to analyze reforming catalyst sintering. Experimental results are illustrated in Figure 24 where crystallite diameter is plotted versus cycle number for multicycle tests using N_2 regeneration at 800°C and 950°C. The initial crystallite diameter of 20nm increased to 32nm after 15 cycles using 950°C regeneration temperature, but increased only to 28nm after 25 cycles using 800°C regeneration temperature. It is interesting to note that crystallite growth at the two regeneration temperatures was almost equal through the first five cycles, to 25nm at 800°C compared to 26nm at 950°C. After 5 cycles, however, relatively little additional crystallite growth occurred at 800°C while significantly more growth occurred at 950°C.

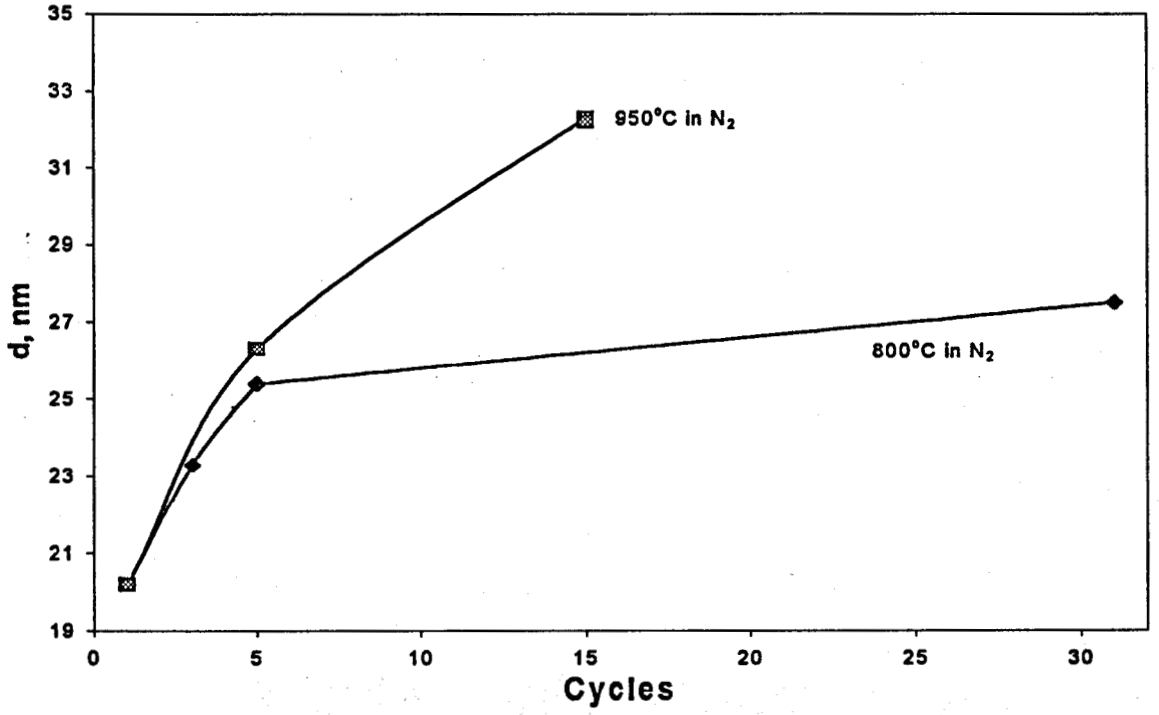

Figure 24. Nickel Crystallite Growth in Multicycle Tests.

Numerous investigators have studied the sintering of calcined limestone and/or calcined dolomite. Of particular relevance to this study, Silaban et al. (1996) reported that dolomite calcined at 750°C in N_2 had a surface area of 21.3m^2/g. After carbonation at 550°C in 15%CO_2/N_2 the surface area decreased to 7 m^2/g, and a second calcination at 750°C in N_2 resulted in a surface area increase only to 16.3m^2/g. Pretreatment, reaction, and regeneration temperatures used in this study were higher, and a limited number of acceptor surface area measurements following the reaction step ($CaCO_3$/MgO) showed that surface area decreased with increasing regeneration temperature and number of cycles. However, difficulties in accurately measuring low surface areas (generally less than 1m^2/g) coupled with limited data made it impossible to reach specific conclusions.

SUMMARY AND CONCLUSIONS

The overall objectives of the research project were accomplished. 95+% H_2 was produced in a single reaction step by adding a calcium-based CO_2 acceptor to standard Ni-based reforming catalyst. The spent acceptor was successfully regenerated and used in a number of reaction steps with only moderate loss in activity as the number of cycles increased. Sufficient experimental data were collected to guide further larger-scale experimental work designed to investigate the economic feasibility of the process.

A more detailed listing of conclusions is presented below organized on the basis of the major topics covered in the body of the report.

Thermodynamic Analysis

1. Reaction equilibrium analysis using HSC Chemistry software showed that production of 95+% H_2 is possible over a range of reaction temperatures, pressures, and feed gas compositions by combining the reforming, shift, and carbonation reactions.

2. An energy balance showed that the combined reactions are approximately thermally neutral, thereby potentially eliminating the need for supplemental energy addition to the primary reactor.

3. The possible formation of $Ca(OH)_2$ may complicate the simultaneous reactions at high pressures and low temperatures. $Ca(OH)_2$ formation is undesirable in that it reduces the amount of acceptor available to react with CO_2 and the concentration of H_2O in the gas phase.

Process Simulation

1. Process simulation using Aspen Plus showed that the single-step process had the potential for producing essentially equivalent H_2 product as conventional steam-methane reforming with an overall energy savings of 20% to 25%.

2. By operating at lower pressure, pure CO2 suitable for sequestration may by produced during the acceptor regeneration step, thereby reducing atmospheric CO2 emissions by almost 60%.

Single Cycle Reaction Studies

1. The experimental work confirmed that the combined reforming, shift, and carbonation reactions are sufficiently fast that combined reaction equilibrium is closely approached at temperatures $\geq 550^{\circ}C$.

2. At equivalent reaction conditions 15 atm and a steam-to-methane ratio of 4 in the feed gas, the ratio of the H_2 content in the presence of the CO_2 acceptor to that without the acceptor ranged from about 3.75 at 450°C to 1.2 at 450°C.

3. Pretreatment to remove sulfur from commercial dolomite is necessary before the dolomite becomes a suitable CO_2 acceptor. Suitable pretreatment conditions were developed.

4. No shift catalysts are required at reaction conditions of interest in the single-step process.

5. H_2 product is available at high pressure ($\geq$ 15 atm), in contrast to membrane reactor H_2 processes currently being studied.

Multicycle Reaction Studies

1. The acceptor can be regenerated at a temperature as low as 800°C in a CO_2-free atmosphere and at 950°C in 1 atm of CO_2.

2. It is not necessary to separate catalyst and acceptor prior to acceptor regeneration.

3. Only modest performance deterioration occurred in 25-cycle tests. Most of the deterioration appears to be associated with the low-cost dolomite ($\approx$1¢ per pound) rather than the more expensive reforming catalyst.

Solids Characterization

1. While the rate of nickel crystallite agglomeration increased with increasing regeneration temperature, sufficient catalyst activity was maintained in all tests to permit postbreakthrough equilibrium to be closely approached.

2. XRD tests using catalyst from long-duration tests showed no evidence of the formation of mixed metal oxide compounds.

3. High temperatures associated with acceptor pretreatment and regeneration caused the acceptor to sinter to final surface areas of about 1 m^2/g.

REFERENCES

Adris, A. M., Pruden, B. B., Lim, C. C., and Grace, J. R., 1996, "On the Reported Attempts to Radically Improve the Performance of the SMR Reactor," *Canadian Journal of Chemical Engineering*, 74, 177.

Agnelli, M. E., Demicheli, M. C., and Ponzi, E. N., 1987, "Catalytic Deactivation of Methane Steam Reforming Catalysts," Ind. Eng. Chem. Res., 26, 1704.

Alzamora, L. E., Ross, J. R., Cruissink, E. C., and VanReijnene, L. R., 1981, "Interactions of Nickel With Alumina Support," *J. Chem. Soc. Farad. Trans. I*, 77, 665.

Anand, M., Hufton, J., Mayorga, S., Sircar, S., and Gaffney, T., 1996, Sorption Enhanced Reaction Process (SERP) for Production of Hydrogen, Proceedings of the 1996 U. S. DOE Hydrogen Program Review, Vol. 1, DE97000053, 537.

Brun-Tsekhovoi, A. R., Zadorin, A. N., Katsobashvili, Y. R., and Kourdumov, S. S., 1988, " The process of Catalytic Steam Reforming of Hydrocarbons in the Presence of CO_2 Acceptor," *Hydrogen Energy Progress, VII, Proceedings of the 7th World Hydrogen Energy Conference*, Pergamon Press.

Eberl, D. D., Drits, V., and Srobon, J., 1996, "MUDMASTER: A Program for Calculating Crystal Size and Size Distributions and Strain from the Shapes of X-ray Diffraction," U. S. Geological Survey, Open File Report.

Gorin, E., and Retallick, W. B., 1963, "Method for the Production of Hydrogen," *U. S. Patent No. 3,108,857.*

Kumar, R., Cole, J., and Lyon, R., 1998, "Unmixed Reforming: An Advanced Steam Reforming Process," presented at the Fuel Cell Reformer Conference, South Coast Air Quality District, Diamond Bar, CA.

Han, C. and Harrison, D. P., 1994, "Simultaneous Wate-Gas Shift Reaction and Carbon Dioxide Separation for Direct Production of H_2 from Synthesis Gas," *Chemical Engineering Science*, 49, 5875.

Han, C. and Harrison, D. P., 1997, "Multicycle Performance of the CO_2 Acceptor in a Single-Step Process for H_2 Production," *Separation Science and Technology*, 32, 681.

Hatano, H., Suzuki, Y., Lin, S., and Harada, M., "Development of Hydrogen Production from Coal with Carbon Dioxide Fixation," Proceedings of the 4th Advanced Clean Coal Technology International Symposium, Tokyo, January 2001.

Lopez Ortiz, A., 2000, "Sorption Enhanced Process for the Production of H_2," Ph. D. Dissertation, Department of Chemical Engineering, Louisiana State University.

Mayorga, S. G., Hufton, J. R., Sircar, S., and Gaffney, T. R., 1997, "Sorption Enhanced Reaction Process for Production of Hydrogen," Phase I Final Report, DOE-Air Products Cooperative Agreement DE-FC36-95-G0010059.

Numaguchi, T., Shoji, K., and Yoshida, S., 1995, "Hydrogen Effect on α-Al_2O_3 Supported Ni Catalysts for SMR Reaction," Appl. Cat., 133, 241.

Roine, A., 1999, "HSC Chemistry 4.1 for Windows, User's Guide," Outompu Research Oy, Finland.

Rostrup-Nielsen, J. R., 1984, "Catalytic Steam Reforming," in *Catalysis Science and Technology,* Anderson, J. R. and Boudart, M. (eds), Springer-Verlag, Berlin.

Silaban, A., Narcida, M., and Harrison, D. P., 1996, "Characteristics of the Reversible Reaction Between CO_2(g) and Calcined Dolomite," *Chemical Engineering Communications,* 147, 149.

Texeira, A. C. and Giudici, R., 1999, "Deactivation of Steam Reforming Catalysts by Sintering: Experiments and Simulation," *Chem. Eng. Sci.,* 54, 3609.

U.S. Department of Energy, National Renewable Energy Laboratory, 1995, Hydrogen Program Overview.

Williams, R., 1933, "Hydrogen Production," *U. S. Patent No. 1,938,202.*

Ziock, H. and Lackner, K., "Overview of the ZECA (Zero Emission Coal Alliance) Technology," Proceedings of the 4th Advanced Clean Coal Technology International Symposium, Tokyo, January 2001.

COMBINING STEAM-METHANE REFORMING, WATER-GAS SHIFT, AND CO_2 REMOVAL IN A SINGLE-STEP PROCESS FOR HYDROGEN PRODUCTION

List of Publications and Presentations

Publications

Hydrogen from Natural Gas in a Single-Step Process
B. Balasubramanian, A. Lopez Ortiz, S. Kaytakoglu, and D. P. Harrison
Chemical Engineering Science, 54, 3543,1999

Hydrogen Production Using Sorption Enhanced Reaction
A. Lopez Ortiz and D. P. Harrison
Industrial and Engineering Chemistry Research, manuscript submitted November 2000

Hydrogen Production in the Presence of a CO_2 Acceptor
A. Lopez Ortiz, B. Balasubramanian, and D. P. Harrison
Proceedings of the 4th Advanced Clean Coal International Symposium, Tokyo, January 2001, p. 293

Presentations

Hydrogen from Natural Gas in a Single-Step Process
B. Balasubramanian, A. Lopez Ortiz, S. Kaytakoglu, and D. P. Harrison
International Symposium on Chemical Reaction Engineering, ISCRE 15, Newport Beach, CA, September 1998

Steam-Methane Reforming in the Presence of a CO_2 Acceptor
B. Balasubramanian, A. Lopez Ortiz, S. Kaytakoglu, and D. P. Harrison
American Institute of Chemical Engineers, Annual Meeting, Miami Beach, November 1998

The Use of Calcined Dolomite as a CO_2 Acceptor in a Single-Step Hydrogen Production Process
A. Lopez Ortiz, J. Yu, and D. P. Harrison
American Institute of Chemical Engineers, Annual Meeting, Dallas, November 2000

Sorption-Enhanced Steam-Methane Reforming
A. Lopez Ortiz and D. P. Harrison
American Institute of Chemical Engineers, Annual Meeting, Los Angeles, November 2001

Hydrogen Production Using Sorption Enhanced Reaction
A. Lopez Ortiz and D. P. Harrison
Engineering Foundation on Chemical Reaction Engineering, Barga, Italy, June 2001 (to be presented)